*Electronic Supporting Information for*

# Heavy-atom-free triplet benzothiophene-fused BODIPY derivatives for lipid droplets-specific biomaging and photodynamic therapy

*Weibin Bu,[a] Changjiang Yu,[a,]* Yingxiu Man,[b] Jiazhu Li,[b,]* Qinghua Wu,[c] Shuangying Gui,[c,]* Yaxiong Wei,[a,]* Lijuan Jiao,[a] and Erhong Hao[a,]**

[a] *The Key Laboratory of Functional Molecular Solids, Ministry of Education, School of Chemistry and Materials Science, School of Physics and Electronic Information, Anhui Normal University, Wuhu 241002, China. E-mail:* yuchj@ahnu.edu.cn, Davidl@mail.ustc.edu.cn, haoehong@ahnu.edu.cn

[b] *College of Chemistry and Chemical Engineering, Yantai University, Yantai, Shandong, China 264005. E-mail:* jiazhu82@ytu.edu.cn

[c] *School of Pharmacy, Anhui University of Chinese Medicine, Hefei 230012, China. E-mail:* guishy0520@126.com

**Contents:**

# 1. General information

Reagents and solvents were used as received from commercial suppliers (Energy Chemicals, Shanghai, China) unless noted otherwise. All reactions were performed in oven-dried or flame-dried glassware unless stated otherwise and were monitored by TLC using 0.25 mm silica gel plates with UV indicator (60F-254). $^{1}H$ and $^{13}C$ NMR spectra were recorded on a 600 MHz NMR spectrometer at room temperature. Chemical shifts (δ) are given in ppm relative to $CDCl_3$ (7.26 ppm for $^{1}H$ and 77 ppm for $^{13}C$) or to internal TMS. High-resolution mass spectra (HRMS) were obtained using MALDI-TOF in positive mode.

**Absorption and emission measurements.**

UV-visible absorption and fluorescence emission spectra were recorded on commercial spectrophotometers (Shimadzu UV-4100 and Edinburgh FS5 spectrometers). All measurements were made at 25 ℃, using 5 × 10 mm cuvettes. Non-degassed, spectroscopic grade solvents and a 10 mm quartz cuvette were used. Absolute fluorescence quantum efficiencies derivatives were measured by absolute PL quantum yield spectrometer (Hamamatsu, C11347) in integrating sphere, using Eq. S1 given below:[1]

$$\Phi_F = \frac{N_{em}}{N_{abs}} = \frac{\alpha \int \frac{\lambda}{hc} I_{em}(\lambda) d\lambda}{\alpha \int \frac{\lambda}{hc} [I_{ex}(\lambda) - I'_{ex}(\lambda)] d\lambda} \qquad \text{Eq. S1}$$

where $N_{em}$ and $N_{abs}$ are the numbers of emitted and absorbed photons, respectively, α is the calibration factor for the measurement setup, λ is the wavelength, h is the Plank's constant, c is the speed of light, $I_{em}(\lambda)$ is the emission intensity at λ, and $Iex(\lambda)$ and $I'_{ex}(\lambda)$ are the intensities of the excitation laser beam with λ in the absence and presence of the sample, respectively. The measured $\Phi_F$ value is independent of sharp and thickness of sample and power of excitation laser.

**Singlet oxygen detection**

A comparative study of the relative singlet oxygen-generating efficiency of these dyes was performed in air-saturated solvents under light at 660 nm or 532 nm laser irradiation (10 mW/cm$^2$) condition using 1,3-diphenylisobenzofuran (DPBF, $4 \times 10^{-5}$ M) as a trap molecule.[2] Established photosensitizers 2,6-diiodobodipy[3] (2I-BDP, $\Phi_\Delta$ = 0.85 in toluene) and methylene blue (MB, $\Phi_\Delta$ = 0.57 in DCM)[4] were used as reference. The absorbance of BODIPY dyes and the references at 532 nm or 635 nm were kept around 0.1-0.25. The decrease of the absorbance band of DPBF at 415 nm was monitored. Singlet oxygen quantum yield ($\Phi_\Delta$) determinations were carried out using the chemical trapping method, and the $\Phi_\Delta$ value was obtained by the relative method using references as the reference as shown in the following equation: $\Phi_{\Delta sam} = \Phi_{\Delta ref}$ $[(m_{sam}/m_{ref})(L_{ref}/L_{sam})]$.

Where $\Phi_{\Delta ref}$ and $\Phi_{\Delta sam}$ are the singlet oxygen quantum yields for the standard references and photosensitizer. $m_{sam}$ and $m_{ref}$ are the slope of the difference ($\Delta$O.D.) in the change in the absorption maximum wavelength of DPBF (415 nm), which are plotted against the photoirradiation time, $L_{ref}$ and $L_{sam}$ are the light harvesting efficiency, which is given by $L = 1\text{-}10^{-A}$ ("A" is the absorbance at the laser irradiation wavelength).

**Preparation of 2a micelle**

Initially, **2a** was dissolved in tetrahydrofuran (THF) to prepare a stock solution with a concentration of 2 mM. Subsequently, 1 mL of chloroform was used as the base liquid, to which 250 μL of the stock solution was added. Following this, 715 μL of tetrahydrofuran solution containing Cremophor EL (40 mg/mL, EL to compound mass ratio of 100:1) was introduced. The mixture was then dried using a rotary evaporator, and finally, 5 mL of deionized water or complete 1640 medium was added to dissolve, yielding a solution (100 μM) for subsequent testing.

**Cell cultures**

HeLa cells were cultured in culture media (RPMI-1640, supplemented with 10% FBS and 1% penicillin/streptomycin solution) at 37 °C in an atmosphere of 5% $CO_2$

and 95% humidified atmosphere. Hepg-2 cells were cultured in Dulbecco's modified Eagle's medium (DMEM) comprised of antibiotics (50 units $mL^{-1}$ penicillin and 50 units $mL^{-1}$ streptomycin) and 10% fetal bovine serum (FBS) at 37 °C in a humidified atmosphere with 5% $CO_2$.

**Cellular uptake studies**

HeLa cells were seeded at a density of $10^6$ cells per well in 96-well cell culture plates and incubated at 37°C with 5% $CO_2$ for 24 hours. **BSBDP 2a** (1 μM) was then added to the wells at different time points, with each column representing a different incubation time. After the incubation period, the remaining liquid was removed, and 100 μL of cell lysate (5% Sodium Dodecyl Sulfate, SDS, PERFEMIKER) was added to each well of the 96-well plate. The cells were completely lysed by shaking the plate, and the fluorescence intensity of the compounds at their emission peaks was detected using an enzyme marker.

**Cellular ROS detection**

HeLa cells were seeded at a density of $10^6$ cells in glass-bottom dishes and incubated at 37°C with 5% $CO_2$ for 24 hours. Then, a solution of **BSBDP 2a** (1 μM) in 1640 complete medium was added to the dishes and incubated for another 24 hours. The culture medium was removed, and the cells were washed three times with PBS. After adding DCFH-DA (2,7-Dichlorofluorescindiacetate, 10 μM) and incubating for 20 minutes, the cells were irradiated with an LED light at 655 ± 10 nm (0.1 $W \cdot cm^{-2}$) for 0.5 hours. The control group was treated with PBS instead of the compound micelles in 1640 solution. Finally, cell imaging was obtained using a confocal laser scanning microscope. The signal of DCF (Dichlorofluorescein, $\lambda_{em}$: 500-550 nm) was collected under laser excitation at 488 nm.

***In vitro* dark cytotoxicity**

The HeLa cells (5000) per well were seeded on 96-well plates and incubated in 1640 complete medium for 24 h at 37 °C. Then, a gradient concentration of **BSBDP 2a** from 0 to 1 μM in a fresh medium was added into the 96-well plate, and the cells with the probe were incubated at 37 °C. Every experiment was performed at least six times.

After 24 h, the working solutions were then removed, and the cells were washed with PBS buffer. A total of 100 μL of CCK-8 (diluted 10-fold, Cell Counting Kit-8, BIOMIKY) was added into each well, and the cells were further incubated at 37 °C for 30 min in a 5% $CO_2$ humidified atmosphere. The plate was shaken for 5 min, and the absorbance was measured at 450 nm using a microplate reader (Multiskan Sky).

**Phototoxicity determined by the CCK-8 method.**

Cells were seeded into 96-well plates with a density of 5000 HeLa cells per well and cultured overnight. Then, a gradient concentration of **BSBDP 2a** in a fresh medium was added to the 96-well plate, and the cells with the NPs were incubated at 37 °C for 12 h. The experimental group of the cells was irradiated with a 655 ± 10 nm LED lamp (0.1 $W \cdot cm^{-2}$) at different times at room temperature. Then these cells were followed by a 12 h incubation solely in the dark (total 24 h) in the incubator. The control groups of the cells were incubated in the dark, for the duration of 24 h under identical experimental conditions except illumination. After that, the working solutions were then removed. A total of 100 μL of CCK-8 (diluted 10-fold, Cell Counting Kit-8, BIOMIKY) was added into each well, and the cells were further incubated at 37 °C for 40 min in a 5% $CO_2$ humidified atmosphere. The plate was shaken for 5 min, and the absorbance was measured at 450 nm using a microplate reader (Multiskan Sky).

**Cellular colocalization imaging.**

A total of 30000 HeLa cells or HepG-2 cells were seeded into a glass bottom dish and were cultured in culture media (RPMI-1640, supplemented with 10% FBS) at 37 °C in an atmosphere of 5% $CO_2$ and 95% humidified atmosphere for 24 h. HeLa cells or HepG-2 cells were first stained with **BSBDP 2a** (1 μM), and Lipi-Blue (0.1 μM) at 37 ºC in an atmosphere of 5% $CO_2$ for 2 h. Then, the morphologies of the cells were observed using a confocal fluorescence microscope (Leica Microsystems SP8 MP, excitation at 638 nm and 405 nm for **BSBDP 2a**, Lipi-Blue, respectively).

**Live–dead cell staining.**

Live–dead cell staining analysis was also performed to evaluate cell viability.

Briefly, a total of 30000 HeLa cells were seeded into a glass bottom dish and were cultured in culture media (RPMI-1640, supplemented with 10% FBS) at 37 °C in an atmosphere of 5% $CO_2$ and 95% humidified atmosphere for 12 h. Cells in control-1 wells were incubated in the incubator for 10 h. Cells in control-2 wells were treated with **BSBDP 2a** (0.2 μM) and were kept in the dark in the same condition for 10 hours. Cells in control-3 were incubated for 10 hours and then illuminated for 1h without the **BSBDP 2a**. Cells in control-4 were incubated with **BSBDP 2a** (0.2 μM) for 10 h, then irradiated for 1 h. The cells were then replaced with AO-PI mixture in the dark at room temperature. After 20 minutes, these plates were taken pictures immediately.

**Animals and Tumor Model.**

All animal studies and the overall project protocols were approved by the Animal Ethics Committee of Anhui University of Chinese Medcine and were in accordance with international guidelines on the ethical use of laboratory animals. The Female BALB/c mice were used as received from commercial suppliers. The accreditation number of the laboratory is SYXK(Zhe) 2019-0004 promulgated by Hangzhou Ziyuan Experimental Animal Technology Co., Ltd. Female BALB/c mice (7-week-old) were maintained in a pathogen free environment under controlled temperature (24 °C). The female mice were injected subcutaneously at left leg with 150 μL of cell suspension containing $1 \times 10^6$ 4T1 cells. The tumors were allowed to grow to ~100 $mm^3$ before experimentation.[5] The tumor volume was calculated as (tumor length) × (tumor width)$^2$/2.

**In *vivo* phototherapy**

**BSBDP 2a** was encapsulated into the amphiphilic block copolymer Pluronic F127 to give nanomicelles (**BSBDP 2a NPs**) for in vivo phototherapy in mice according to our previous report.[6] When the tumor volume reached about 100 $mm^3$, tumor-bearing mice were divided into four groups (n = 4 mice/group) randomly for different formulations[7]: (1) PBS; (2) **BSBDP 2a NPs**; (3) **BSBDP 2a NPs** + Laser. The solution of different groups (100 μL, 0.5 mg $mL^{-1}$) was intravenously injected into mice and irradiated by the 660 nm laser (0.2 W $cm^{-2}$) for 10 min after 24 h. The tumor dimensions (length and width) and body weight were measured every two days after the treatment. The mice were sacrificed after 2 weeks post-treatment, the tumors, and major organs including heart, liver, spleen, lung, kidney were collected, and photos were taken.

## 2. Synthesis and characterization

*Synthesis of ethyl 7-formyl-8-isopropyl-1-methylthieno[3,2-e]indole-2-carboxylate* ***3a***

Anhydrous DMF (1.61 mL, 20.88 mmol) was placed to a pre-dried round bottom flask and cooled in an ice bath, then $POCl_3$ (1.27 mL, 13.92 mmol) was added dropwise under $N_2$ atmosphere. The mixture was warmed to room temperature and stirred for 1 h, and a solution of ethyl 8-isopropyl-1-methylthieno[3,2-*e*]indole-2-carboxylate (2.11 g, 7.0 mmol) in DMF (15 mL) was added dropwise. The reaction mixture was refluxed with stirring overnight and then poured into crushed ice. After neutralizing with a base, the mixture was extracted with dichloromethane (DCM). The organic layer was separated, dried with anhydrous $Na_2SO_4$, and removed under reduced pressure. The solid residue was purified by silica gel column chromatography (DCM: Hexane = 1: 1) to obtain the desired compound **3a** as a light yellow solid (761 mg, 33%). mp: 231.0-232.4 ℃. $^1$H NMR (600 MHz, $CDCl_3$) δ 10.35 (s, 1H), 9.58 (s, 1H), 7.68 (d, *J* = 8.7 Hz, 1H), 7.46 (d, *J* = 8.7 Hz, 1H), 4.41 (q, *J* = 7.1 Hz, 2H), 4.16-4.05 (m, 1H), 3.06 (s, 3H), 1.61 (d, *J* = 7.1 Hz, 6H), 1.43 (t, *J* = 7.1 Hz, 3H). $^{13}$C NMR (151 MHz, $CDCl_3$) δ 181.7, 163.6, 141.5, 136.7, 136.4, 136.1, 135.2, 131.8, 128.0, 122.2, 122.1, 113.6, 61.3, 27.8, 27.4, 19.0, 14.5. HRMS (ESI): calcd for $C_{18}H_{20}NO_3S^+$ 330.1158; found *m/z* 330.1170 ($[M+H]^+$).

*Synthesis of 8-isopropyl-1-methylthieno[3,2-e]indole-7-carbaldehyde* ***3b***

Compound **3a** (500 mg, 1.52 mmol) was dissolved in THF (20 mL). Methanol (10 mL), LiOH (1.5 g) in water (10 mL) was then added. The mixture was refluxed with stirring for 2.5 h and then poured into crushed ice. The pH was adjusted to 2-3 by adding diluted HCl, and then the mixture was extracted with ethyl acetate. The organic phase was separated, dried with anhydrous $Na_2SO_4$, and removed under reduced pressure to give an orange solid. To the solid in DMF (10 mL) was added $Cu_2O$ (0.1 g). After refluxing at 160 °C for 3 h, the mixture was poured into crushed ice, and then extracted with DCM (3 × 100 mL). The organic phase was separated, dried with anhydrous $Na_2SO_4$, and removed under reduced pressure. The solid residue was purified by silica gel column chromatography (DCM : hexane = 2 : 1) to obtain the desired compound

**3b** as light yellow solid (312 mg, 1.22 mmol, 80%). mp: 190.6-191.3 ℃. $^{1}$H NMR (600 MHz, $CDCl_3$) δ 10.36 (s, 1H), 9.59 (s, 1H), 7.73 (d, *J* = 8.7 Hz, 1H), 7.35 (d, *J* = 8.7 Hz, 1H), 7.26 (s, 1H), 4.38-4.23 (m, 1H), 2.82 (s, 3H), 1.62 (d, *J* = 7.2 Hz, 6H). $^{13}$C NMR (151 MHz, $CDCl_3$) δ 181.9, 136.5, 136.4, 136.3, 133.8, 133.1, 131.3, 125.0, 123.0, 122.1, 110.4, 27.3, 20.9. HRMS (ESI): calcd for $C_{15}H_{16}NOS^+$ 258.0947; found *m/z* 258.0958 ($[M+H]^+$).

*General procedure for the preparation of BODIPYs* ***BBDP 1a*** *and* ***BBDP 1b***

To the mixture of compound **3** (5 mmol, 1 equiv.) and 2,4-dimethyl-1*H*-pyrrole (1 equiv.) in anhydrous DCM (100 mL) in an ice bath was added $POCl_3$ (1.1 equiv.) dropwise under $N_2$ atmosphere. The reaction mixture was warmed to room temperature and stirred overnight. Upon the completion of the reaction, saturated $NaHCO_3$ (100 mL) was added, and the mixture was left stirring for additional 10 min. Organic layer was separated, dried with anhydrous $Na_2SO_4$, and removed under reduced pressure. The solid residue was then dissolved in anhydrous toluene (100 mL). Then, DIPEA (5.0 mL) and $BF_3{\cdot}OEt_2$ (5.0 mL) were added successively under ice-cold condition through syringe. The reaction mixture was warmed to 100 °C and stirred for 1 h, poured into water and extracted with DCM. Organic layers were combined, dried with anhydrous $Na_2SO_4$, and removed under reduced pressure. The crude product was purified by silica gel chromatography (eluting with DCM) to afford the desired compounds.

**BBDP 1a**: dark red solid, 33%. mp: 254.3-255.2 ℃. $^{1}$H NMR (600 MHz, $CDCl_3$) δ 7.82 (d, *J* = 8.9 Hz, 1H), 7.63 (s, 1H), 7.61 (d, *J* = 8.9 Hz, 1H), 6.26 (s, 1H), 4.39 (q, *J* = 7.1 Hz, 2H), 4.13-4.04 (m, 1H), 2.98 (s, 3H), 2.67 (s, 3H), 2.34 (s, 3H), 1.57 (d, *J* = 7.2 Hz, 6H), 1.42 (t, *J* = 7.1 Hz, 3H). $^{13}$C NMR (151 MHz, $CDCl_3$) δ 165.0, 163.5, 146.3, 145.9, 142.1, 141.7, 138.1, 137.1, 134.6, 132.9, 127.8, 124.9, 124.2, 123.6, 122.8, 116.3, 61.2, 28.2, 26.8, 18.9, 15.6, 14.5, 11.7. $^{11}$B NMR (128 MHz, $CDCl_3$) δ 1.14 (t, *J* = 32.3 Hz). $^{19}$F NMR (376 MHz, $CDCl_3$) δ -145.56 (dd, *J* = 64.6, 31.8 Hz). HRMS (ESI): calcd for $C_{24}H_{25}BFN_2O_2S^+$ 435.1708; found *m/z* 435.1724 ($[M-F]^+$).

**BBDP 1b**: dark red solid, 60%. mp: > 300 ℃. $^{1}$H NMR (600 MHz, $CDCl_3$) δ 7.70 (d, *J* = 9.0 Hz, 1H), 7.66 (d, *J* = 8.8 Hz, 1H), 7.65 (s, 1H), 7.19 (s, 1H), 6.24 (s, 1H), 4.29-

4.21 (m, 1H), 2.76 (s, 3H), 2.66 (s, 3H), 2.34 (s, 3H), 1.58 (d, $J$ = 7.2 Hz, 6H). $^{13}$C NMR (151 MHz, $CDCl_3$) δ 163.8, 146.9, 145.2, 142.4, 137.7, 136.6, 133.9, 133.2, 132.6, 125.4, 125.2, 125.2, 123.6, 122.4, 113.1, 27.6, 26.7, 20.8, 15.5, 11.6. $^{11}$B NMR (128 MHz, $CDCl_3$) δ 1.19 (t, $J$ = 32.6 Hz). $^{19}$F NMR (376 MHz, $CDCl_3$) δ -145.92 (dd, $J$ = 65.1, 32.4 Hz). HRMS (ESI): calcd for $C_{21}H_{21}BFN_2S^+$ 363.1497; found *m/z* 363.1512 ($[M-F]^+$).

*General procedure for the preparation of BODIPYs* ***BSBDP 2a*** *and* ***BSBDP 2b***

To BODIPY **1** (0.15 mmol) and corresponding benzaldehyde derivatives (0.20 mmol) in anhydrous toluene (20 mL) was added piperidine (0.14 mL) and acetic acid (0.11 mL) through syringe. The reaction mixture was left heated at 140 °C under nitrogen, during which time the water was removed with a Soxhlet extractor containing anhydrous $CaCl_2$. The reaction was monitored by TLC. Upon the disappearance of **1**, the reaction mixture was cooled down to room temperature, poured into water and extracted with DCM (3 × 50 mL). Organic layers were combined and dried over anhydrous $Na_2SO_4$. Solvent was removed under vacuum. The crude product was purified by chromatography (eluting with hexane : DCM = 1 : 1 or DCM) to afford the desired BODIPY **2**.

**BSBDP 2a:** dark green solid, 69%. mp: > 300 ℃. $^1$H NMR (600 MHz, $CDCl_3$) δ 7.88 (d, $J$ = 8.9 Hz, 1H), 7.68 – 7.58 (m, 4H), 7.53 (s, 1H), 7.43 (d, $J$ = 16.2 Hz, 1H), 6.94 (d, $J$ = 8.3 Hz, 2H), 6.84 (s, 1H), 4.40 (q, $J$ = 7.1 Hz, 2H), 4.11-4.05 (m, 1H), 3.87 (s, 3H), 3.00 (s, 3H), 2.38 (s, 3H), 1.58 (d, $J$ = 7.1 Hz, 6H), 1.42 (t, $J$ = 7.2 Hz, 3H). $^{13}$C NMR (151 MHz, $CDCl_3$) δ 163.7, 161.8, 160.7, 145.8, 144.5, 142.2, 141.7, 140.2, 139.8, 137.1, 134.5, 133.5, 130.2, 128.7, 127.6, 125.0, 123.5, 120.8, 118.7, 116.6, 116.3, 114.7, 61.17, 55.6, 28.2, 26.6, 19.0, 14.5, 11.8. $^{11}$B NMR (128 MHz, $CDCl_3$) δ 1.45 (t, $J$ = 32.9 Hz). $^{19}$F NMR (376 MHz, $CDCl_3$) δ -142.01 (dd, $J$ = 64.5, 30.4 Hz). HRMS (ESI): calcd for $C_{32}H_{31}BFN_2O_3S^+$ 553.2127; found *m/z* 553.2127 ($[M-F]^+$).

**BSBDP 2b:** dark brown solid, 63%. mp: >300 ℃. $^1$H NMR (600 MHz, $CDCl_3$) δ 7.77 (d, $J$ = 8.8 Hz, 1H), 7.67 (d, $J$ = 8.9 Hz, 1H), 7.64 (d, $J$ = 16.2 Hz, 1H), 7.60 (d, $J$ = 8.4 Hz, 2H), 7.54 (s, 1H), 7.39 (d, $J$ = 16.2 Hz, 1H), 7.18 (s, 1H), 6.93 (d, $J$ = 8.2 Hz, 2H),

6.81 (s, 1H), 4.32-4.24 (m, 1H), 3.86 (s, 3H), 2.76 (s, 3H), 2.35 (s, 3H), 1.59 (d, $J$ = 7.2 Hz, 6H). $^{13}$C NMR (151 MHz, $CDCl_3$) δ 161.6, 159.7, 146.3, 143.9, 140.9, 140.8, 139.4, 136.5, 133.9, 133.1, 130.0, 128.9, 125.3, 125.0, 124.8, 121.0, 118.4, 116.7, 114.6, 113.1, 55.6, 27.6, 26.6, 20.8, 11.7. $^{11}$B NMR (128 MHz, $CDCl_3$) δ 1.48 (t, $J$ = 33.0 Hz). $^{19}$F NMR (376 MHz, $CDCl_3$) δ -142.35 (dd, $J$ = 65.5, 31.3 Hz). HRMS (ESI): calcd for $C_{29}H_{27}BFN_2OS^+$ 481.1916; found *m/z* 481.1932 ($[M-F]^+$).

## 3. Crystal diagrams and selected parameters

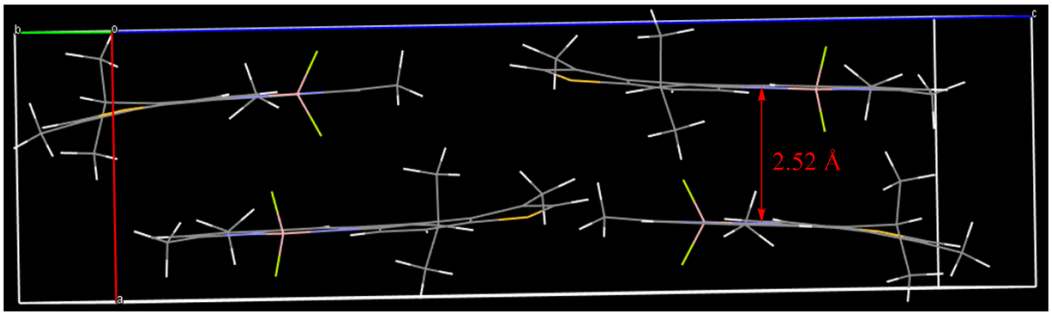


**Figure S1.** Crystal packing of **BBDP 1b** (interlay distance is 2.52 Å).

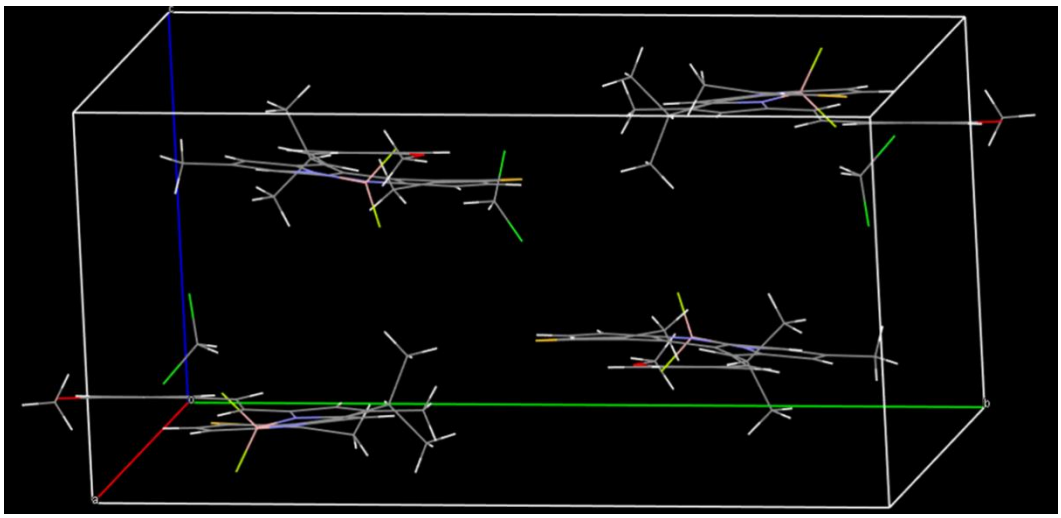

**Figure S2.** Crystal plot and packing of **BSBDP 2b**.

**Table S1.** Selected bond lengths and dihedral angles of **BBDP 1b** and **BSBDP 2b**.

| | | |
|---|---|---|
| B-N bond distances (Å) | 1.541, 1.537 | 1.538, 1.557 |
| B-F bond distances (Å) | 1.377, 1.395 | 1.386, 1.394 |
| dihedral angles between five-membered thiophene ring A and the BODIPY core (deg) | 7.87(2) | 7.19 (2) |
| dihedral angles between six-membered benzo ring B and the BODIPY core (deg) | 2.98(2) | 5.67(1) |
| dihedral angles between the pyrrolyl ring C and the BODIPY core (deg) | 0.89(2) | 4.96(1) |
| dihedral angles between the formed six-membered $C_3N_2B$ ring D and the BODIPY core (deg) | 0.36(2) | 1.41(1) |
| dihedral angles between the ring E and the BODIPY core (deg) | 0.19(2) | 4.66(1) |
| dihedral angles between the phenyl ring F (deg) and the BODIPY core (deg) | - | 5.14(1) |
| dihedral angles between thiophene core A and phenyl ring B (deg) | 4.89(3) | 5.25(1) |
| dihedral angles between pyrrolyl ring C and the six-membered $C_3N_2B$ ring D (deg) | 1.24(3) | 4.61(1) |
| dihedral angles between pyrrolyl ring C and the pyrrolyl ring E (deg) | 0.97(3) | 9.60(2) |

## 4. Spectroscopic properties

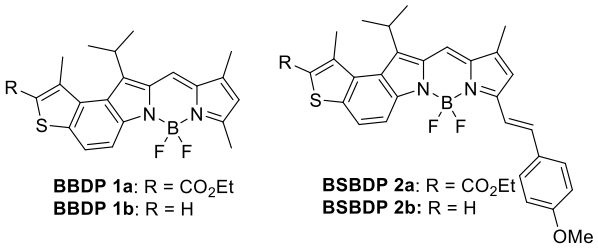


**Table S2.** Photophysical properties of **BBDPs 1a**, **1b**, **BSBDPs 2a** and **2b** in toluene and singlet oxygen formation quantum yields in solvents.

| BODIPYs | $\lambda_{abs}^{max}$ (nm)[a] | log$\varepsilon_{max}$[b] | $\lambda_{em}^{max}$ (nm) | $\Phi_F$[c] | $\tau_F$ (ns)[d] | $\tau_\Delta$(μs)[e] | $\Phi_\Delta$[f] | $\Phi_\Delta$[g] | $\Phi_\Delta$[h] |
|---|---|---|---|---|---|---|---|---|---|
| **BBDP 1a** | 571 | 4.92 | 587 | 0.04 | 1.35 | 320 | 0.72 | - | - |
| **BBDP 1b** | 572 | 4.99 | 605 | 0.04 | 1.04 | - | 0.49 | - | - |
| **BSBDP 2a** | 645 | 4.99 | 672 | 0.23 | 1.63 | 154 | - | 0.69 | 0.45 |
| **BSBDP 2b** | 645 | 4.99 | 666 | 0.25 | 1.42 | - | - | 0.71 | 0.32 |

[a] All of values are corrected for changes in refractive indexes of toluene. [b] Molar absorption coefficients are in the maximum of the highest peak. [c] Absolute fluorescence quantum yields. [d] Fluorescence lifetime. [e] Triplet state lifetime.[f] Singlet oxygen formation quantum yield in toluene. [g] Singlet oxygen formation quantum yield in dichloromethane. [h] Singlet oxygen formation quantum yield in MeOH.

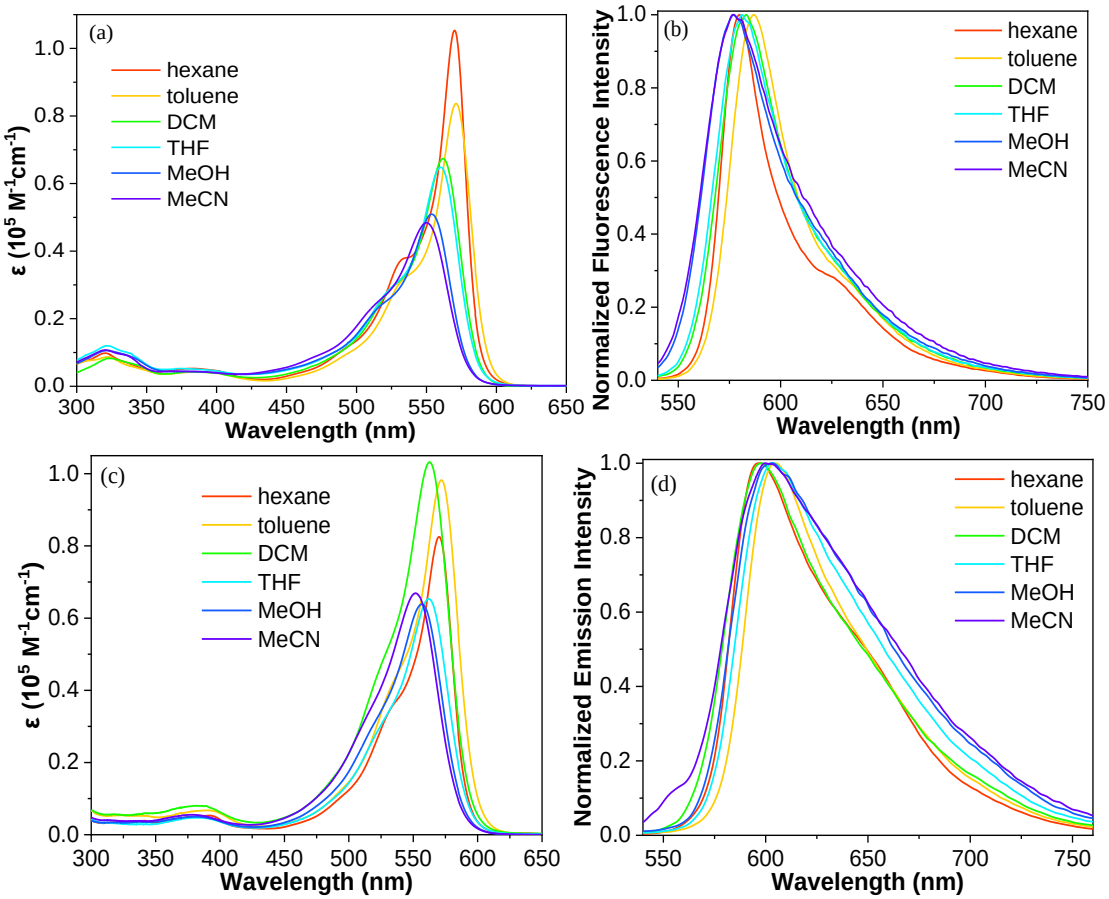


**Figure S3.** Overlaidabsorption and normalized emission spectra of **BBDPs 1a** (a) and **1b** (b) in six common organic solvents, excited at 520 nm.

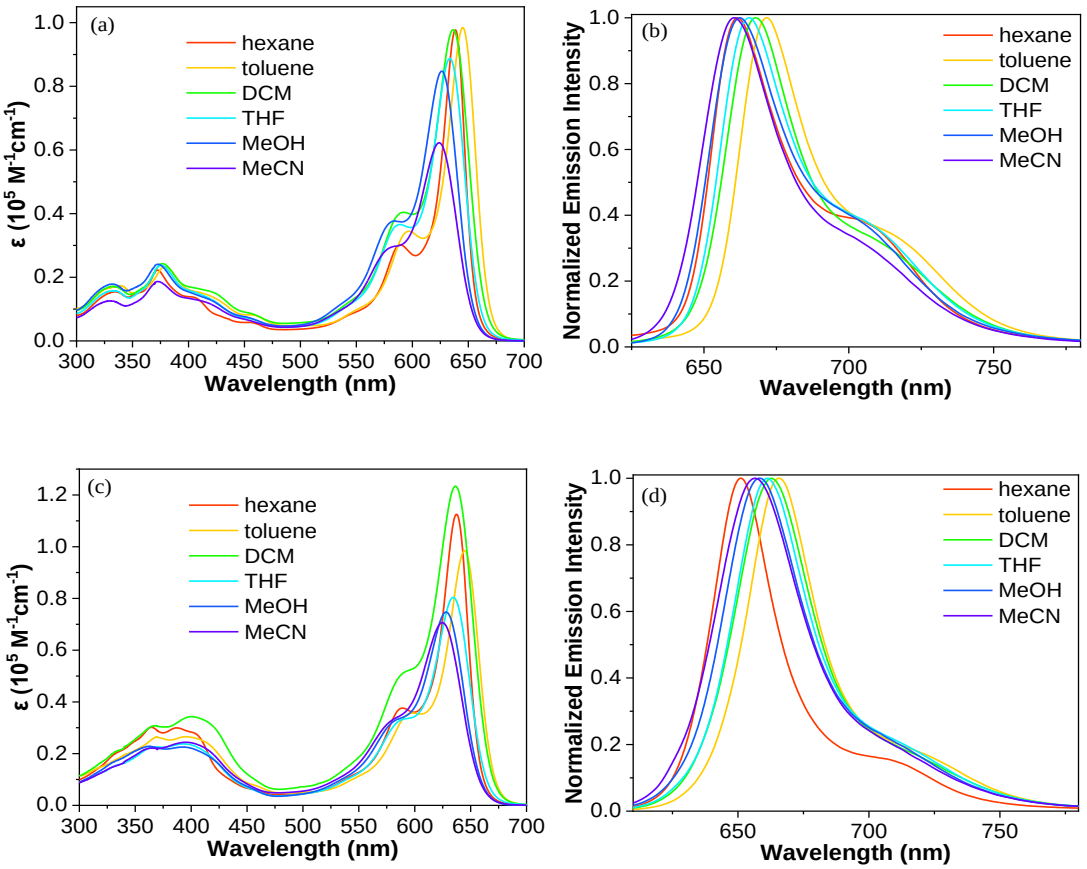


**Figure S4.** Overlaid absorption and normalized emission spectra of **BSBDPs 2a** (a) and **2b** (b) in six common organic solvents, excited at 600 nm.

**Table S3.** Photophysical properties of **BBDPs 1a-b** and **BSBDPs 2a-b** in different solvents at room temperature.

| BODIPYs | solvents | $\lambda_{abs}^{max}$ (nm)[a] | $\log\varepsilon_{max}$[b] | $\lambda_{em}^{max}$ (nm) | $\Phi$[c] | $\tau$[d] (ns) | Stokes Shift (nm) |
|---|---|---|---|---|---|---|---|
| **BBDP 1a** | hexane | 570 | 5.18 | 580 | 0.04 | 1.40 | 10 |
| | toluene | 571 | 4.92 | 587 | 0.04 | 1.35 | 16 |
| | DCM | 562 | 4.83 | 583 | 0.03 | 1.04 | 21 |
| | THF | 560 | 4.81 | 581 | 0.03 | 1.12 | 21 |
| | MeOH | 554 | 4.71 | 577 | 0.02 | 0.88 | 23 |
| | MeCN | 550 | 4.68 | 577 | 0.01 | 0.83 | 27 |
| **BBDP 1b** | hexane | 570 | 4.92 | 597 | 0.06 | 1.51 | 27 |
| | toluene | 572 | 4.99 | 605 | 0.04 | 1.04 | 33 |
| | DCM | 563 | 5.01 | 598 | 0.03 | 0.66 | 35 |
| | THF | 562 | 4.82 | 604 | 0.03 | 0.71 | 42 |
| | MeOH | 557 | 4.80 | 603 | 0.02 | 0.39 | 46 |
| | MeCN | 552 | 4.83 | 600 | 0.01 | 0.38 | 48 |

| | | | | | | | |
|---|---|---|---|---|---|---|---|
| **BSBDP 2a** | hexane | 638 | 4.99 | 662 | 0.16 | 1.22 | 24 |
| | toluene | 645 | 4.99 | 672 | 0.30 | 1.63 | 27 |
| | DCM | 636 | 4.99 | 668 | 0.32 | 1.60 | 32 |
| | THF | 633 | 4.95 | 666 | 0.31 | 1.62 | 33 |
| | MeOH | 626 | 4.93 | 662 | 0.28 | 1.55 | 36 |
| | MeCN | 624 | 4.79 | 660 | 0.32 | 1.60 | 36 |
| **BSBDP 2b** | hexane | 637 | 5.05 | 651 | 0.25 | 1.35 | 14 |
| | toluene | 645 | 4.99 | 666 | 0.25 | 1.42 | 21 |
| | DCM | 637 | 5.09 | 663 | 0.21 | 1.25 | 26 |
| | THF | 635 | 4.91 | 661 | 0.21 | 1.23 | 26 |
| | MeOH | 628 | 4.87 | 658 | 0.17 | 0.89 | 30 |
| | MeCN | 625 | 4.85 | 656 | 0.14 | 0.81 | 31 |

[a]All of values are corrected for changes in refractive indexes of different solvents. [b]Molar absorption coefficients are in the maximum of the highest peak. [c]The absolute fluorescence quantum yields (Φ) for these dyes were measured on Edinburgh FLS 1000 fluorescence spectrometer by integrating sphere. The standard errors are less than 5%. [d]Fluorescence lifetime; standard deviations are less than 0.1 ns.

## 5. Singlet oxygen production yield measurement

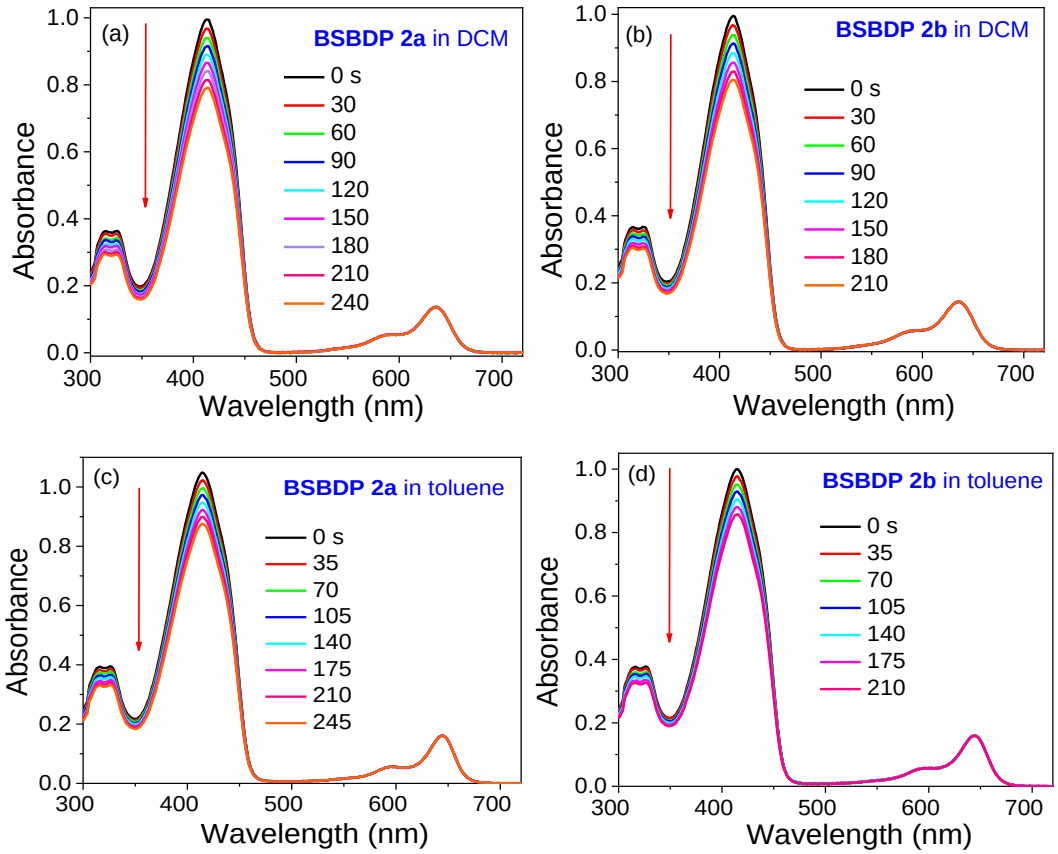

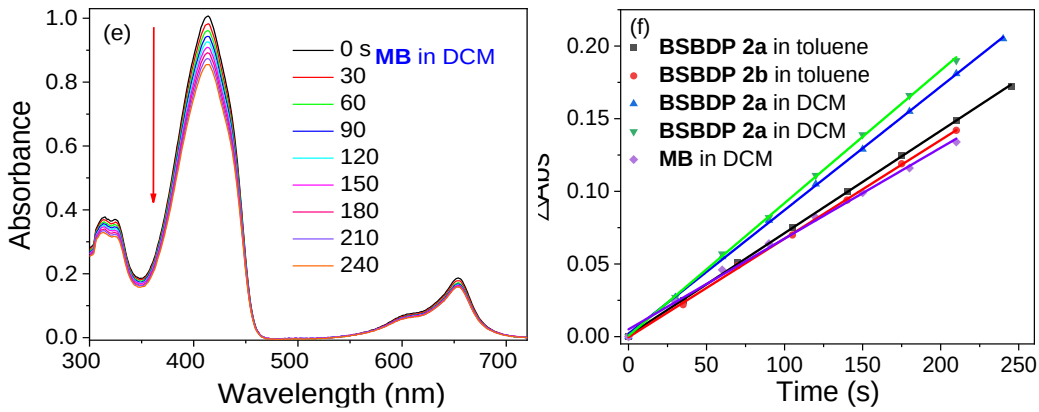


**Figure S5.** Absorption spectra of DPBF (initial absorbance around 1.0 around 414 nm) upon irradiation in the presence of **BSBDP 2a** and **BSBDP 2b** in dichloromethane (DCM) and toluene with initial absorbance around 0.15 at 635 nm. (a) **BSBDP 2a** for 240 s (recorded at 30 s intervals) in DCM; (b) **BSBDP 2b** for 210 s (recorded at 30 s intervals) in DCM; (c) **BSBDP 2a** for 245 s (recorded at 30 s or 35 s intervals) in toluene; (d) **BSBDP 2b** for 210 s (recorded at 35 s intervals) in toluene; (e) **MB** for 240 s (recorded at 30 s intervals) in DCM. (f) Plot of change in absorbance of DPBF at 414 nm vs irradiation time in the presence of **BSBDP 2a-b** in DCM and toluene against MB in dichloromethane as the standard.

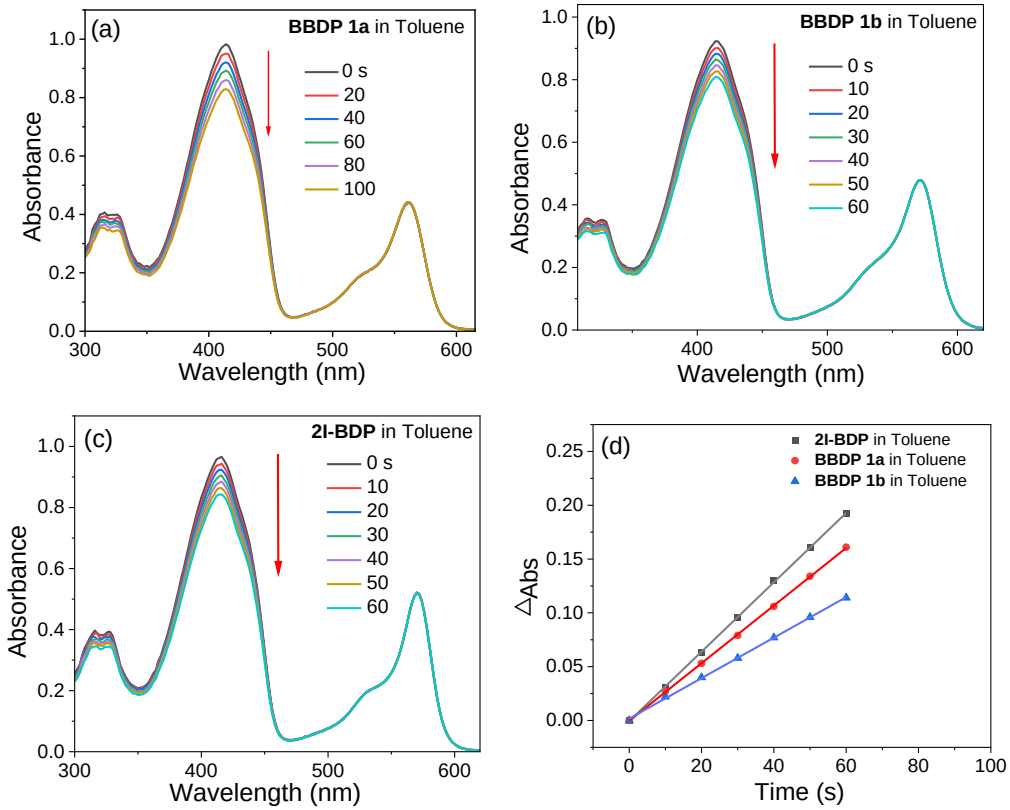

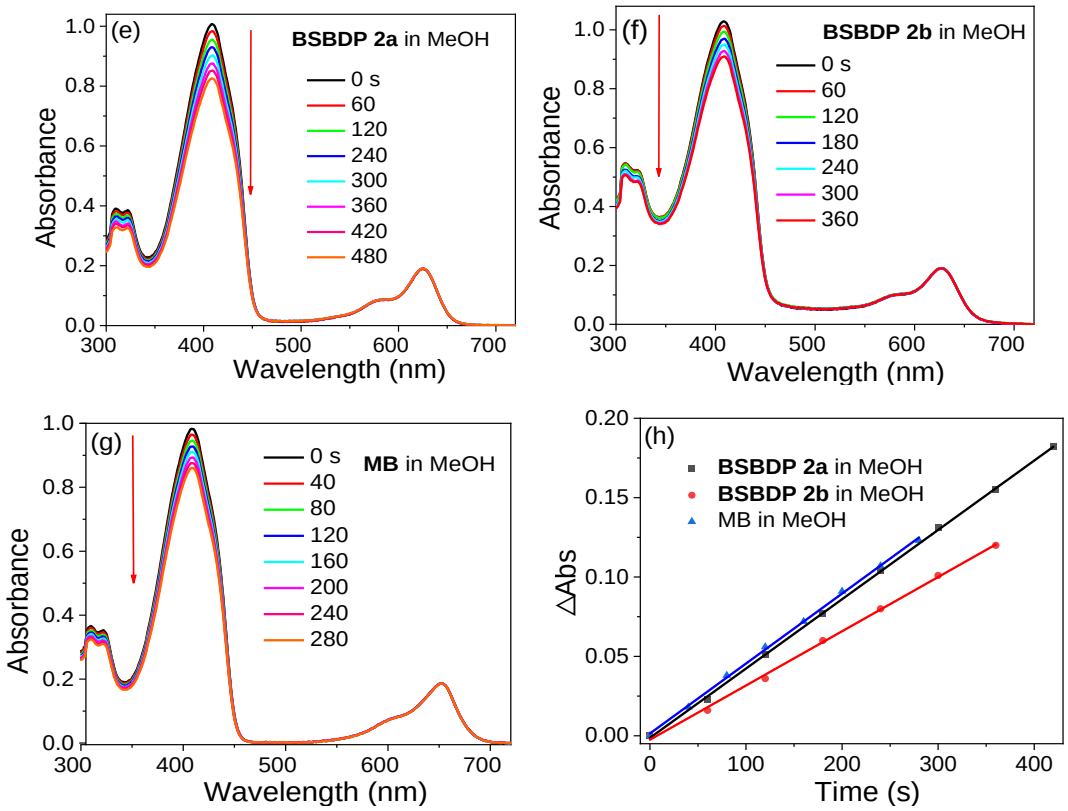


**Figure S6.** Absorption spectra of DPBF (initial absorbance around 1.05 at 414 nm) upon irradiation in the presence of **1a** and **1b** with initial absorbance around 0.2 at 532 nm. (a) Reference 2I-BDP for 60 s (recorded at 20 s intervals) in toluene ; (b) **1a** for 100 s (recorded at 10 s intervals) in toluene; (c) **1b** for 120 s (recorded at 10 s intervals) in toluene; (d) Plot of changes in absorbance of DPBF at 414 nm vs irradiation time in the presence of **1a** and **1b** against 2I-BDP as the standard in toluene and dichloromethane. Absorption spectra of DPBF upon irradiation in the presence of **2a** and **2b** in methanol at 635 nm. (e) **2a** for 480 s (recorded at 60 s intervals); (f) **2b** for 360 s (recorded at 60 s intervals); (g) **MB** for 280 s (recorded at 40 s intervals). (h) Plot of change in absorbance of DPBF at 414 nm vs irradiation time in the presence of **2a-b** in methanol against **MB** in methanol as the standard.

## 6. Density functional theory calculations

The ground state geometry was optimized by using DFT method at B3LYP/6-31G(d) level. The same method was adopted for vibrational analysis to verify that the optimized structures correspond to local minima on the energy surface. TD-DFT computations were used the optimized ground state geometries under the B3LYP/6-31G(d,p) theoretical level. The molecule calculation in dichloromethane were using the Self-Consistent Reaction Field (SCRF) method and Polarizable Continuum Model (PCM). All of the calculations for **1** and **2** were carried out by thmethods implemented in Gaussian 09 package.[8]

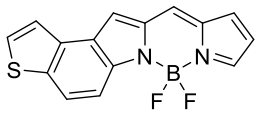


**1**

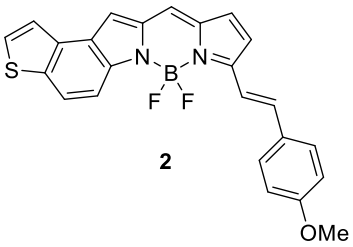


**2**

**Table S4.** Selected electronic excitation energies (eV) and oscillator strengths (*f*), configurations of the low-lying singlet excited states of **1** and **2** skeletons calculated by TDDFT//B3LYP/6–31G (d, p), based on the optimized ground state geometries.

| | Electronic transition | TD//B3LYP/6-31G(d, p) | | | |
|---|---|---|---|---|---|
| | | Energy/ eV [a] | *f* [b] | Composition [c] | CI [d] |
| **1** | S0→S1 | 2.2783 eV 544.20 nm | 0.0984 | HOMO → LUMO | 0.4329 |
| | | | | HOMO -1 → LUMO | 0.5571 |
| | S0→S2 | 2.5434 eV 487.48 nm | 0.8262 | HOMO -2 → LUMO | 0.1016 |
| | | | | HOMO -1 → LUMO | 0.4295 |
| | | | | HOMO → LUMO | 0.5534 |
| | S0→S3 | 3.3927 eV 365.45 nm | 0.1326 | HOMO -2 → LUMO | 0.6813 |
| | | | | HOMO -3 → LUMO | 0.1072 |
| **2** | S0→S1 | 2.0810 eV 595.80 nm | 1.4712 | HOMO → LUMO | 0.7067 |
| | S0→S2 | 2.2898 eV 541.47 nm | 0.0359 | HOMO -1 → LUMO | 0.6949 |
| | | | | HOMO -2 → LUMO | 0.1054 |
| | S0→S3 | 2.8199 eV 439.68 nm | 0.1609 | HOMO -2 → LUMO | 0.6784 |
| | | | | HOMO → LUMO + 1 | 0.1516 |

[a] Only the selected low-lying excited states are presented. [b] Oscillator strength. [c] Only the main configurations are presented. [d] The CI coefficients are in absolute values.

**Table S5.** Selected electronic excitation energies (eV) and oscillator strengths (*f*), configurations of the low-lying triplet excited states of **1** and **2** skeletons calculated by TDDFT//B3LYP/6–31G (d, p), based on the optimized ground state geometries.

| | Electronic transition | TD//B3LYP/6-31G(d, p) | | | |
|---|---|---|---|---|---|
| | | Energy/ eV [a] | *f* [b] | Composition [c] | CI [d] |
| **1** | S0→T1 | 1.3191 eV 939.91 nm | 0.0000 | HOMO -2 → LUMO | 0.1601 |
| | | | | HOMO → LUMO | 0.6920 |
| | | | | HOMO ← LUMO | 0.1154 |
| | S0→T2 | 1.8574 eV 667.50 nm | 0.0000 | HOMO -1 → LUMO | 0.6947 |
| | S0→T3 | 2.6461 eV 468.55 nm | 0.0000 | HOMO -2 → LUMO | 0.5472 |
| | | | | HOMO -3 → LUMO | 0.3211 |
| | | | | HOMO → LUMO | 0.1375 |
| | | | | HOMO → LUMO + 1 | 0.1509 |
| **2** | S0→T1 | 1.0828 eV 1144.99 nm | 0.0000 | HOMO -3 → LUMO | 0.1244 |
| | | | | HOMO → LUMO | 0.7003 |
| | | | | HOMO ← LUMO | 0.1282 |
| | S0→T2 | 1.8531 eV 669.06 nm | 0.0000 | HOMO -1 → LUMO | 0.6803 |
| | | | | HOMO -6 → LUMO | 0.1005 |
| | S0→T3 | 2.1949 eV 564.88 nm | 0.0000 | HOMO -2 → LUMO | 0.6565 |
| | | | | HOMO → LUMO + 1 | 0.1844 |

[a] Only the selected low-lying excited states are presented. [b] Oscillator strength. [c] Only the main configurations are presented. [d] The CI coefficients are in absolute values.

**Table S6.** Lowest vertical singlet and triplet electronic transition energies (in eV) and oscillator strengths (in parentheses) of **1** and **2** at the TD-B3LYP levels, along with vertical singlet-triplet splittings (in eV) and SOCs between the involved S1 and T1 states (in $cm^{-1}$).

| dyes | state/assignment[a] | TD-B3LYP | $\Delta E_{S_1-T_n}$ | $\langle S_1\|\hat{H}_{SO}\|T_n\rangle$[b] | $k_{ISC}$ |
|---|---|---|---|---|---|
| **1** | $S_1$ (H→L, c = 0.43; H -1→L, c = 0.56) | 2.278 (0.0984) | - | | |
| | $T_1$ (H→L, c = 0.69; H -2→L, c = 0.16; H ← L, c = 0.11) | 1.319 | 0.959 | 0.05 | 0.0025 |
| | $T_2$ (H -1→L, c = 0.69) | 1.857 | 0.421 | 0.49 | 1.35 |
| **2** | $S_1$ (H→L, c = 0.69) | 2.081 (1.4712) | - | | |
| | $T_1$ (H→L, c = 0.70; H -3→L, c = 0.12; H ← L, c = 0.13) | 1.083 | 0.998 | 0.88 | 0.77 |
| | $T_2$ (H -1→L, c = 0.68; H -6→2, c = 0.10) | 1.853 | 0.228 | 0.32 | 1.96 |

[a]Only the first excited states are considered. [b]Values are shown as (x component; y component; z component) and were obtained at the QR-TD-DFT/6-31G* level of theory at the T1 optimized geometry.

DFT optimized coordinates for **1** optimized $S_0$ state Geometry by B3LYP/6-31G(d).

| | | | |
|---|---|---|---|
| S | -5.05262500 | -0.49143500 | -0.09301100 |
| F | 1.90736900 | -2.11631900 | -0.80906500 |
| F | 2.01818400 | -1.67786500 | 1.42979000 |
| N | 3.27618900 | -0.25488700 | -0.06910000 |

| | | | |
|---|---|---|---|
| N | 0.79173800 | -0.12722800 | 0.02374400 |
| C | -4.99746400 | 1.24873300 | -0.00674000 |
| H | -5.92253100 | 1.80986500 | 0.00529700 |
| C | -3.72407700 | 1.73643100 | 0.03890900 |
| C | -2.73361100 | 0.70188500 | 0.00611300 |
| C | -3.30109800 | -0.58267100 | -0.06712000 |
| C | -2.52633400 | -1.76969200 | -0.11946400 |
| H | -3.02010200 | -2.73447700 | -0.18638800 |
| C | -1.14722300 | -1.70368100 | -0.09460500 |
| H | -0.54102700 | -2.59973900 | -0.15317100 |
| C | -0.53835500 | -0.43093500 | -0.01004400 |
| C | -0.38675400 | 1.83916900 | 0.09764000 |
| C | -1.30707700 | 0.78507000 | 0.03643300 |
| C | 0.89877000 | 1.25915000 | 0.08580200 |
| C | 2.15394100 | 1.88115400 | 0.07185000 |
| H | 2.20596800 | 2.96447100 | 0.10638500 |
| C | 3.32373000 | 1.14265700 | -0.02263200 |
| C | 4.68427800 | 1.54227800 | -0.14659900 |
| C | 5.43723100 | 0.38609500 | -0.27273700 |
| H | 6.50813100 | 0.30454600 | -0.39659300 |
| C | 4.53049500 | -0.69948400 | -0.21777500 |
| B | 1.98360600 | -1.11576200 | 0.15460500 |
| H | -3.49465500 | 2.79472700 | 0.09472800 |
| H | -0.58892200 | 2.90134600 | 0.13235800 |
| H | 5.03391200 | 2.56617700 | -0.15357600 |
| H | 4.73903400 | -1.75964100 | -0.27712200 |

SCF done: -1309.43838887 a.u.

No imaginary Frequency.

DFT optimized coordinates for **1** optimized $S_1$ state Geometry by B3LYP/6-31G(d).

| | | | |
|---|---|---|---|
| S | -5.05262500 | -0.49143500 | -0.09301100 |
| F | 1.90736900 | -2.11631900 | -0.80906500 |
| F | 2.01818400 | -1.67786500 | 1.42979000 |
| N | 3.27618900 | -0.25488700 | -0.06910000 |
| N | 0.79173800 | -0.12722800 | 0.02374400 |
| C | -4.99746400 | 1.24873300 | -0.00674000 |
| H | -5.92253100 | 1.80986500 | 0.00529700 |
| C | -3.72407700 | 1.73643100 | 0.03890900 |
| C | -2.73361100 | 0.70188500 | 0.00611300 |
| C | -3.30109800 | -0.58267100 | -0.06712000 |
| C | -2.52633400 | -1.76969200 | -0.11946400 |
| H | -3.02010200 | -2.73447700 | -0.18638800 |
| C | -1.14722300 | -1.70368100 | -0.09460500 |
| H | -0.54102700 | -2.59973900 | -0.15317100 |

| | | | |
|---|---|---|---|
| C | -0.53835500 | -0.43093500 | -0.01004400 |
| C | -0.38675400 | 1.83916900 | 0.09764000 |
| C | -1.30707700 | 0.78507000 | 0.03643300 |
| C | 0.89877000 | 1.25915000 | 0.08580200 |
| C | 2.15394100 | 1.88115400 | 0.07185000 |
| H | 2.20596800 | 2.96447100 | 0.10638500 |
| C | 3.32373000 | 1.14265700 | -0.02263200 |
| C | 4.68427800 | 1.54227800 | -0.14659900 |
| C | 5.43723100 | 0.38609500 | -0.27273700 |
| H | 6.50813100 | 0.30454600 | -0.39659300 |
| C | 4.53049500 | -0.69948400 | -0.21777500 |
| B | 1.98360600 | -1.11576200 | 0.15460500 |
| H | -3.49465500 | 2.79472700 | 0.09472800 |
| H | -0.58892200 | 2.90134600 | 0.13235800 |
| H | 5.03391200 | 2.56617700 | -0.15357600 |
| H | 4.73903400 | -1.75964100 | -0.27712200 |

SCF done: -1309.36271794 a.u.

No imaginary Frequency.

DFT optimized coordinates for **2** optimized $S_0$ state Geometry by B3LYP/6-31G(d).

| | | | |
|---|---|---|---|
| S | -6.92399400 | -2.64131400 | -0.10041800 |
| F | -0.08690100 | -0.58347800 | -0.55901800 |
| F | -0.32164200 | 0.05164200 | 1.62405900 |
| N | 0.14932200 | 1.78259600 | -0.00565300 |
| N | -2.07454900 | 0.64788500 | 0.05585100 |
| C | -7.75589200 | -1.10796400 | -0.14868000 |
| H | -8.83700900 | -1.09123500 | -0.18971700 |
| C | -6.90399000 | -0.04375400 | -0.12779600 |
| C | -5.52549500 | -0.43527100 | -0.07030500 |
| C | -5.36523700 | -1.83344700 | -0.04929600 |
| C | -4.09809200 | -2.46480800 | 0.00180100 |
| H | -4.03202300 | -3.54864800 | 0.00719400 |
| C | -2.94448700 | -1.70364200 | 0.03741000 |
| H | -1.96705300 | -2.17064900 | 0.05919300 |
| C | -3.06595300 | -0.29647900 | 0.02763900 |
| C | -4.08406000 | 1.74254100 | -0.03639900 |
| C | -4.34155500 | 0.36066100 | -0.03010400 |
| C | -2.68769600 | 1.89460000 | 0.01535400 |
| C | -1.90651800 | 3.06508700 | -0.01900700 |
| H | -2.39913100 | 4.03087900 | -0.05371300 |
| C | -0.52796500 | 3.00385400 | -0.04371400 |
| C | 0.44326000 | 4.04793100 | -0.14999000 |
| C | 1.67908800 | 3.45443400 | -0.17649600 |
| H | 2.63660300 | 3.94689700 | -0.27098100 |

| | | | |
|---|---|---|---|
| C | 1.48185300 | 2.03294600 | -0.08139400 |
| B | -0.56257100 | 0.41403200 | 0.29735100 |
| H | -7.24040200 | 0.98701000 | -0.15126300 |
| H | -4.79842600 | 2.55348000 | -0.08646000 |
| H | 0.21328000 | 5.10331500 | -0.21516100 |
| C | 2.46688100 | 0.98859500 | -0.07981500 |
| H | 2.08379700 | -0.02496700 | -0.10503500 |
| C | 3.80667200 | 1.22189300 | -0.05879000 |
| H | 4.15135300 | 2.25448600 | -0.03785900 |
| C | 4.86775500 | 0.23138800 | -0.05658300 |
| C | 6.20659300 | 0.66678400 | -0.04642900 |
| C | 4.63646400 | -1.16530200 | -0.06212200 |
| C | 7.27481300 | -0.22617300 | -0.04413200 |
| H | 6.41488300 | 1.73389300 | -0.04074400 |
| C | 5.68641200 | -2.06385700 | -0.05965200 |
| H | 3.62105600 | -1.54873200 | -0.06583000 |
| C | 7.01864800 | -1.60474800 | -0.05092000 |
| H | 8.28912500 | 0.15467600 | -0.03675500 |
| H | 5.50756600 | -3.13451800 | -0.06295800 |
| O | 7.97225200 | -2.56911200 | -0.04870200 |
| C | 9.34395800 | -2.17333900 | -0.03663500 |
| H | 9.91911900 | -3.09980300 | -0.03581300 |
| H | 9.59526900 | -1.58687400 | -0.92793600 |
| H | 9.58145600 | -1.59386400 | 0.86296800 |

SCF done: -1732.43718763 a.u.
No imaginary Frequency.

DFT optimized coordinates for **2** optimized $S_1$ state Geometry by B3LYP/6-31G(d).

| | | | |
|---|---|---|---|
| S | -6.92399400 | -2.64131400 | -0.10041800 |
| F | -0.08690100 | -0.58347800 | -0.55901800 |
| F | -0.32164200 | 0.05164200 | 1.62405900 |
| N | 0.14932200 | 1.78259600 | -0.00565300 |
| N | -2.07454900 | 0.64788500 | 0.05585100 |
| C | -7.75589200 | -1.10796400 | -0.14868000 |
| H | -8.83700900 | -1.09123500 | -0.18971700 |
| C | -6.90399000 | -0.04375400 | -0.12779600 |
| C | -5.52549500 | -0.43527100 | -0.07030500 |
| C | -5.36523700 | -1.83344700 | -0.04929600 |
| C | -4.09809200 | -2.46480800 | 0.00180100 |
| H | -4.03202300 | -3.54864800 | 0.00719400 |
| C | -2.94448700 | -1.70364200 | 0.03741000 |
| H | -1.96705300 | -2.17064900 | 0.05919300 |
| C | -3.06595300 | -0.29647900 | 0.02763900 |
| C | -4.08406000 | 1.74254100 | -0.03639900 |

| | | | |
|---|---|---|---|
| C | -4.34155500 | 0.36066100 | -0.03010400 |
| C | -2.68769600 | 1.89460000 | 0.01535400 |
| C | -1.90651800 | 3.06508700 | -0.01900700 |
| H | -2.39913100 | 4.03087900 | -0.05371300 |
| C | -0.52796500 | 3.00385400 | -0.04371400 |
| C | 0.44326000 | 4.04793100 | -0.14999000 |
| C | 1.67908800 | 3.45443400 | -0.17649600 |
| H | 2.63660300 | 3.94689700 | -0.27098100 |
| C | 1.48185300 | 2.03294600 | -0.08139400 |
| B | -0.56257100 | 0.41403200 | 0.29735100 |
| H | -7.24040200 | 0.98701000 | -0.15126300 |
| H | -4.79842600 | 2.55348000 | -0.08646000 |
| H | 0.21328000 | 5.10331500 | -0.21516100 |
| C | 2.46688100 | 0.98859500 | -0.07981500 |
| H | 2.08379700 | -0.02496700 | -0.10503500 |
| C | 3.80667200 | 1.22189300 | -0.05879000 |
| H | 4.15135300 | 2.25448600 | -0.03785900 |
| C | 4.86775500 | 0.23138800 | -0.05658300 |
| C | 6.20659300 | 0.66678400 | -0.04642900 |
| C | 4.63646400 | -1.16530200 | -0.06212200 |
| C | 7.27481300 | -0.22617300 | -0.04413200 |
| H | 6.41488300 | 1.73389300 | -0.04074400 |
| C | 5.68641200 | -2.06385700 | -0.05965200 |
| H | 3.62105600 | -1.54873200 | -0.06583000 |
| C | 7.01864800 | -1.60474800 | -0.05092000 |
| H | 8.28912500 | 0.15467600 | -0.03675500 |
| H | 5.50756600 | -3.13451800 | -0.06295800 |
| O | 7.97225200 | -2.56911200 | -0.04870200 |
| C | 9.34395800 | -2.17333900 | -0.03663500 |
| H | 9.91911900 | -3.09980300 | -0.03581300 |
| H | 9.59526900 | -1.58687400 | -0.92793600 |
| H | 9.58145600 | -1.59386400 | 0.86296800SCF done: -1732.36920322 a.u. |

No imaginary Frequency.

## 7. Cellular experiments

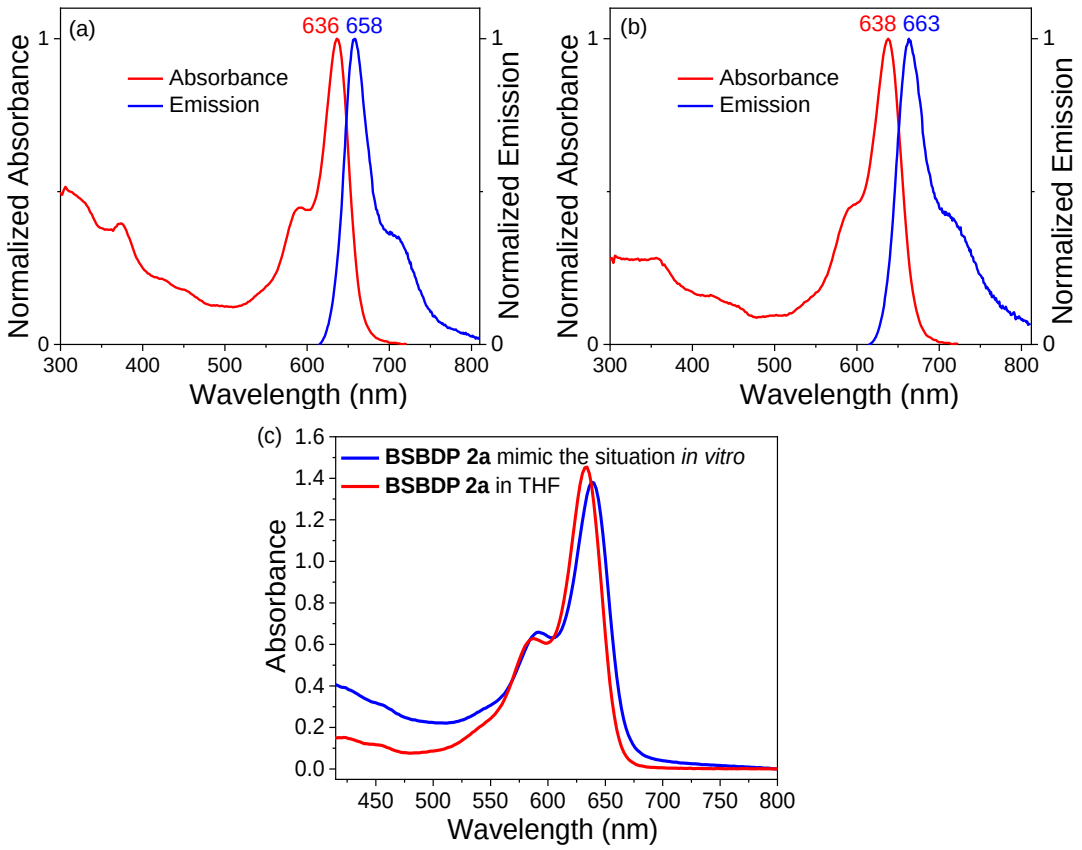


**Figure S7.** Normalized absorption and emission spectra of **2a** (a) and **2b** (b) with 100 eq Cremophor EL in water. (c) Absorption spectra of **BSBDP 2a** (30 μM) in THF or mixture with 150 eq Cremophor EL in water.

## Optimization of imaging conditions

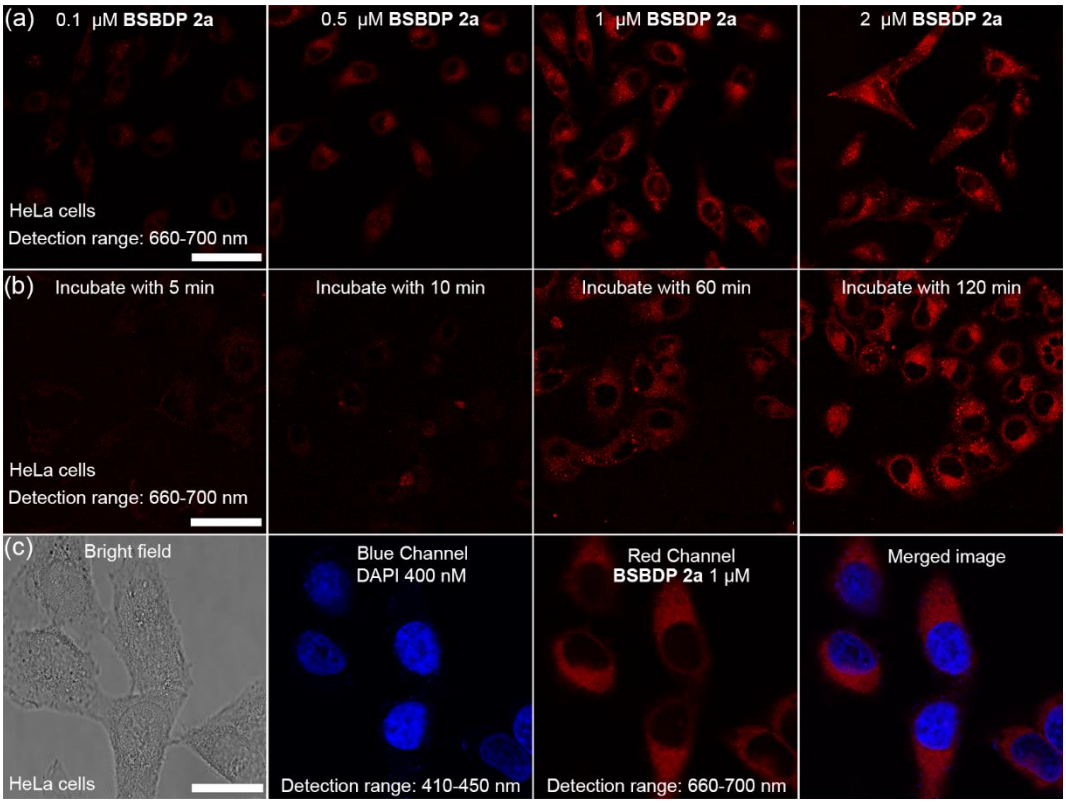


**Figure S8.** (a) Fluorescence images of different concentrations of **BSBDP 2a** incubated with HeLa cell for 2h, Scale bars = 25 μm**;** (b) Fluorescence images of **BSBDP 2a** (1 μM) incubated with HeLa cells at different times, Scale bars = 25 μm.; (c) Fluorescence images of **BSBDP 2a** and DAPI incubated with HeLa cells, **BSBDP 2a** (1 μM) fluorescence after incubation for 2h, DAPI (400 nM) fluorescence after incubation for 30 min, Scale bars = 10 μm.

## Cell uptake study.

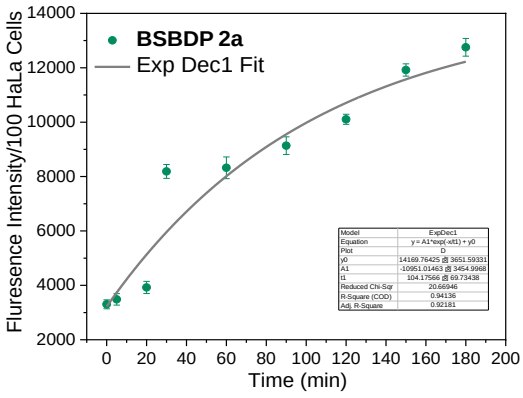


**Figure S9.** Fluorescent intensity of **BSBDP 2a** ($\lambda_{ex}$ = 638 nm; 1 μM) incubated with HeLa cells at different times.

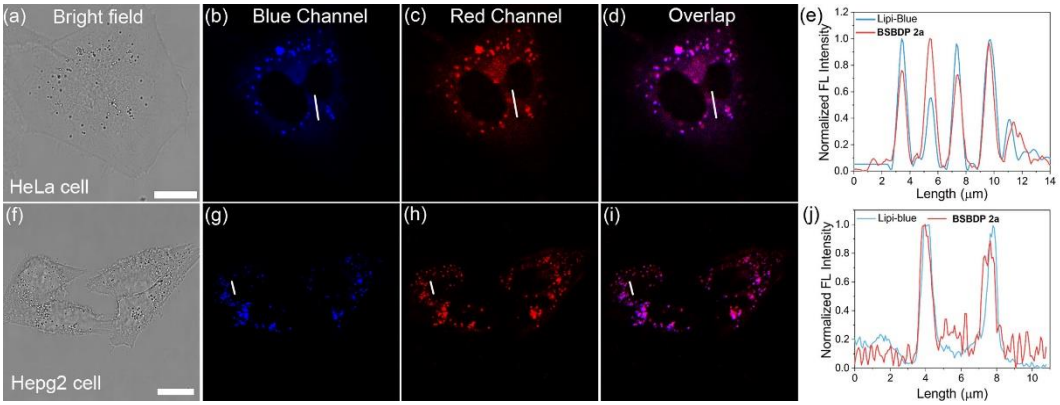


**Figure S10.** LD co-localization studies of **BSBDP 2a** in HeLa cells and Hepg2 cell. (a,f) Bright field. (b,g) Lipi-Blue fluorescence (0.1 μM, LD commercial dye) fluorescence, $\lambda_{ex}$ = 405 nm, $\lambda_{em}$: 420-460 nm. (c,h) **BSBDP 2a** (1 μM) fluorescence, $\lambda_{ex}$ = 638 nm, $\lambda_{em}$: 660-700 nm. (d,i) Merged images of Blue Channel and Red Channel. (e,j) Intensity profiles within the regions of interest of **BSBDP 2a** and Lipi-Blue across HeLa cells or Hepg2 cells, Pearson's correlation Rr = 0.91 or 0.86.

## DCFH-DA detects intracellular ROS

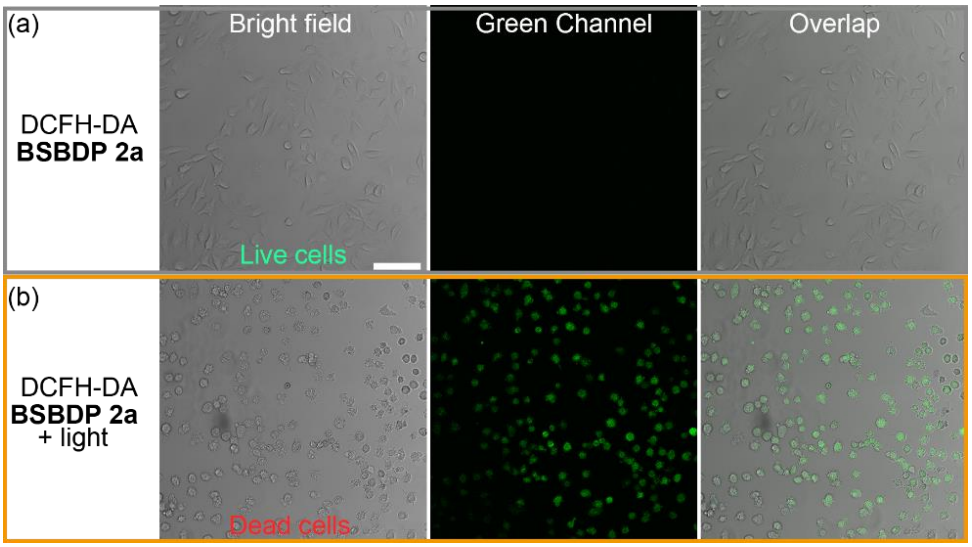


**Figure S11.** Fluorescence imaging of ROS detection with/without **BSBDP 2a** (0.2 μM) and light irradiation (655 ± 10 nm, 40 J $cm^{-2}$) in HeLa cells and DCFH-DA (10 μM) was used as the fluorescence detector.

## Cytotoxicity study

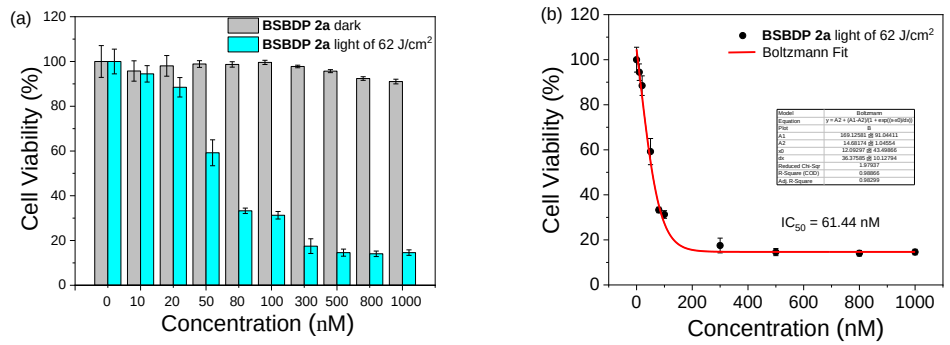


**Figure S12.** (a) Cell suspensions were seeded in 96-well flat-bottom plates and varying concentrations of the sensitizers were added to each well. HeLa cells were kept either in the dark, or under illumination with a red LED lamp (655 ± 10 nm) for a period of 47 min at 37 °C. (b) Curve fitting between the cell viability and the concentration of **BSBDP 2a**. $IC_{50}$ = 61.44 nM.

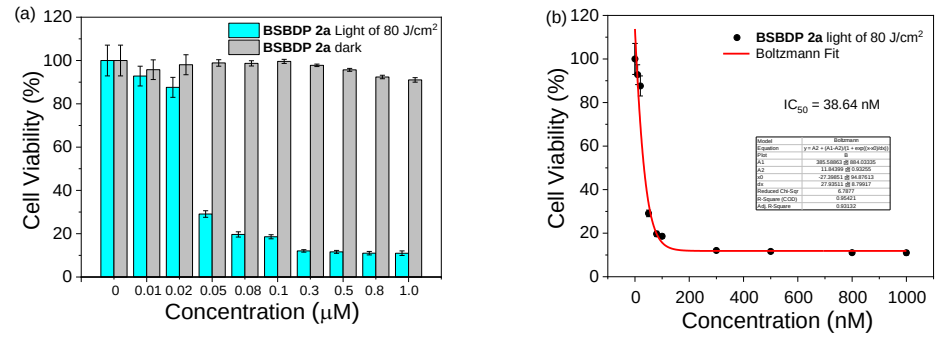


**Figure S13.** (a) Cell suspensions were seeded in 96-well flat-bottom plates and varying concentrations of the sensitizers were added to each well. HeLa cells were kept either in the dark, or under illumination with a red LED lamp (655 ± 10 nm) for a period of 1 h at 37 °C. (b) Curve fitting between the cell viability and the concentration of **BSBDP 2a**. $IC_{50}$ = 38.64 nM.

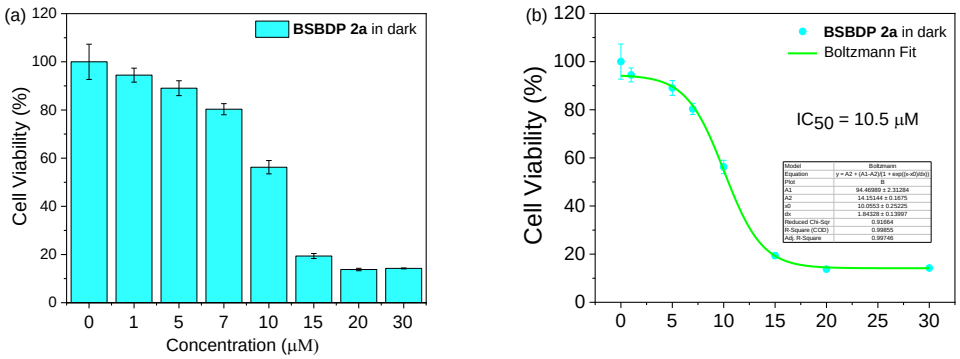


**Figure S14.** (a) Cytotoxicity of HeLa cells treated with different concentrations of **BSBDP 2a** for 24 h as demonstrated by CCK-8 assay. (b) Curve fitting between the cell viability and the concentration of **BSBDP 2a**. $IC_{50}$ = 10.5 μM.

## 8. In vivo phototherapy

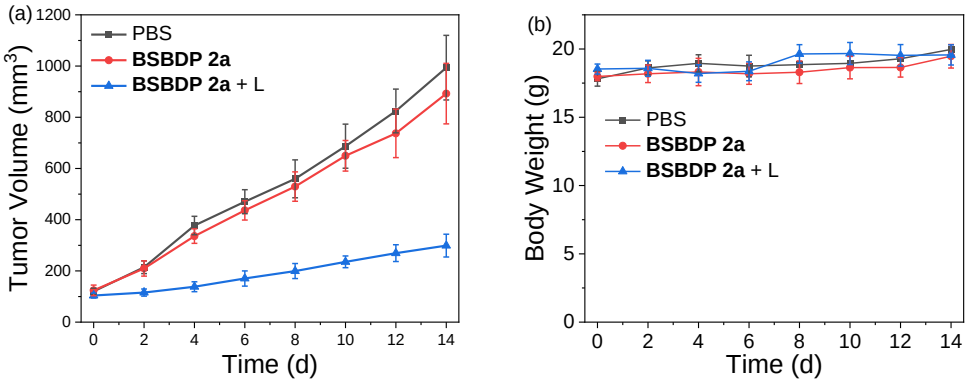


**Figure S15.** (a) Tumor volumes of different groups of mice. (b) Body weight of different groups of mice.

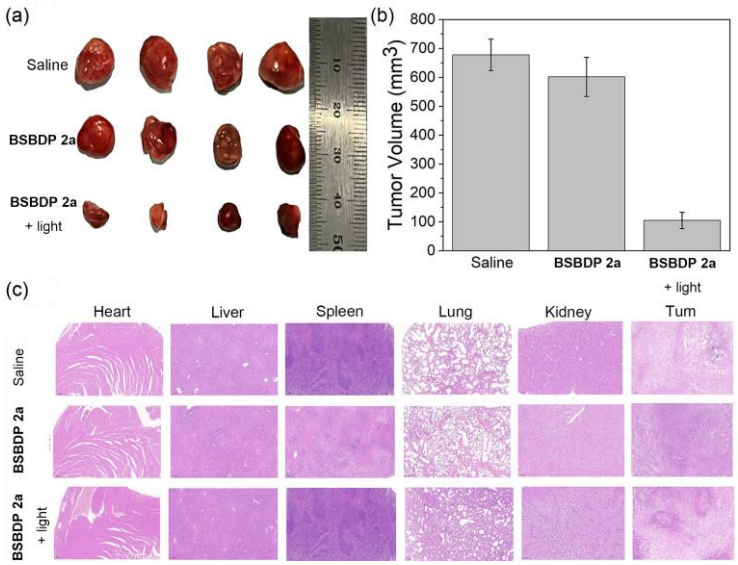


**Figure S16.** (a) Photographs of mouse tumors after 14 days of different treatment modalities; (b) Tumor volumes of mice in different treatment groups after 14 days (n=4 per group, $p < 0.01$). (c) H&E staining of different organs and tumor sections from different groups after 14 days of treatment. Scale bar: 100 μm.

# 9. NMR spectra for all the new compounds

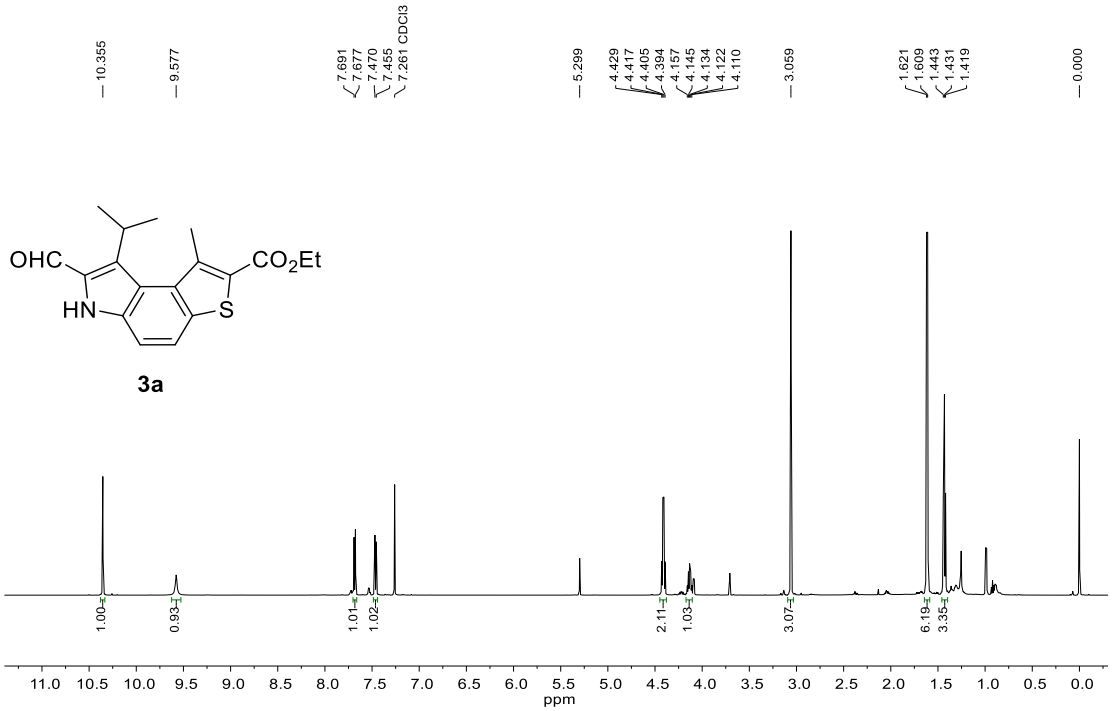


$^{1}$H NMR spectrum of compound **3a** in $CDCl_3$

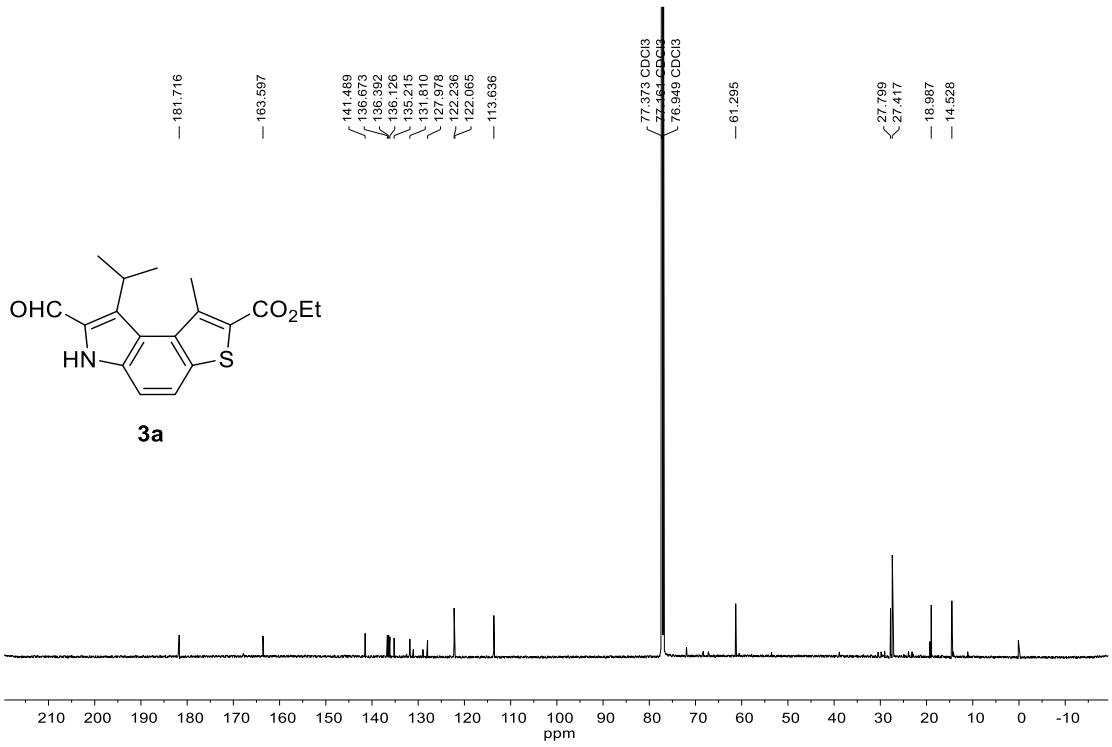


$^{13}$C NMR spectrum of compound **3a** in $CDCl_3$

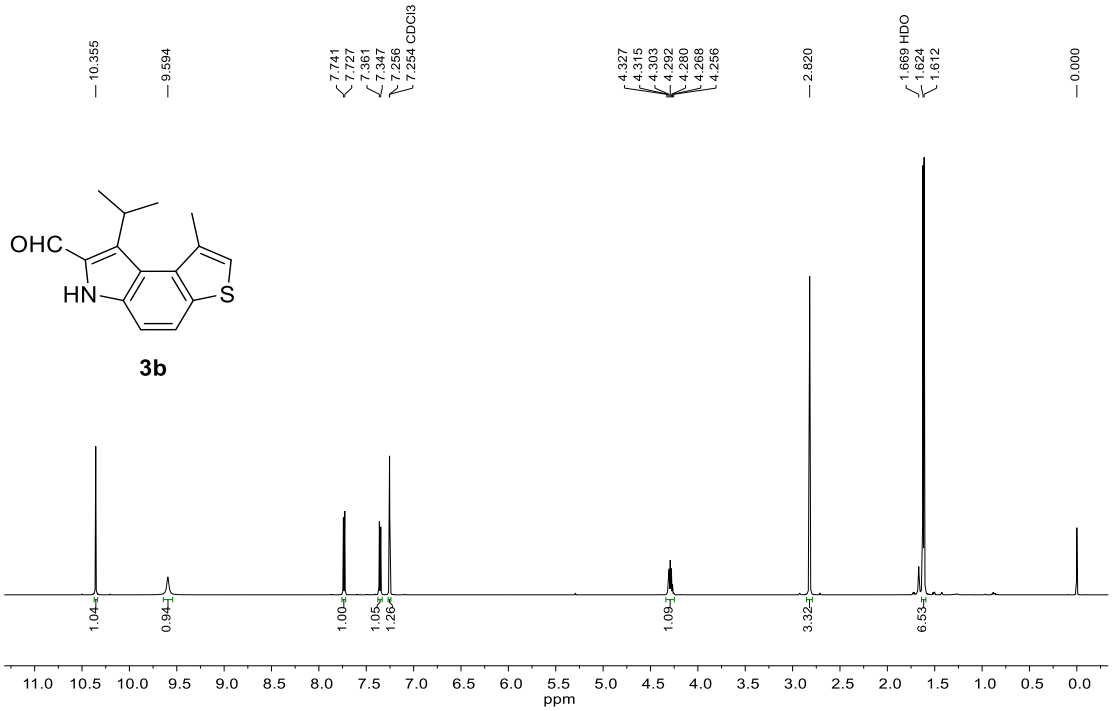


$^{1}$H NMR spectrum of compound **3b** in $CDCl_3$

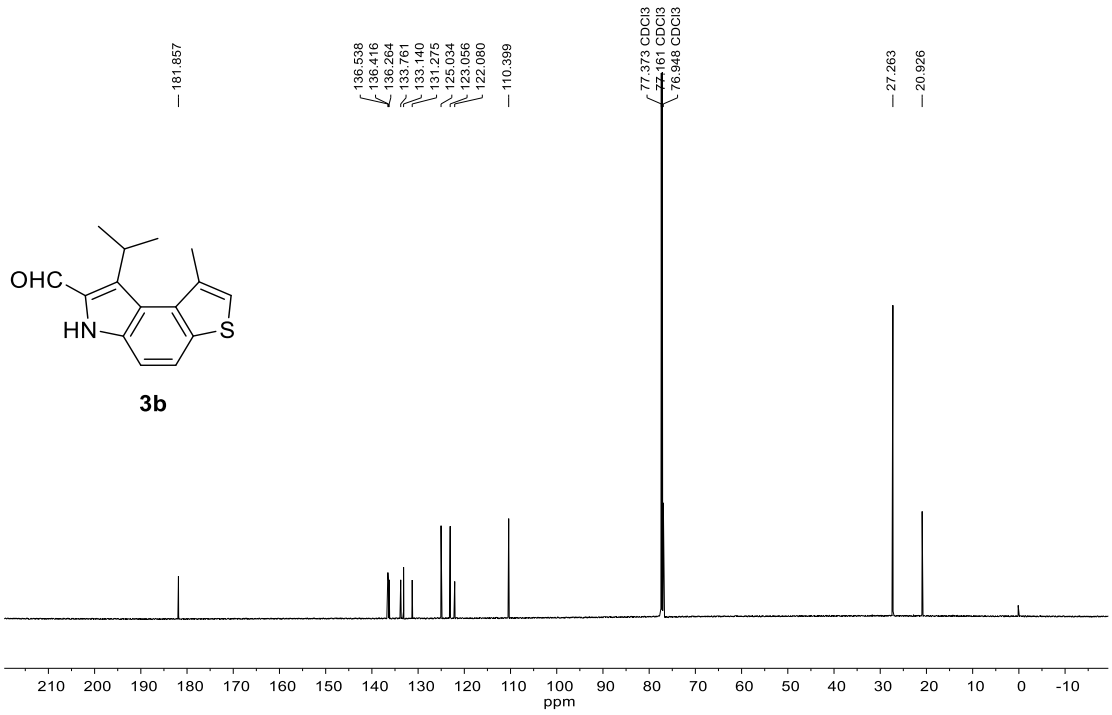


$^{13}$C NMR spectrum of compound **3b** in $CDCl_3$

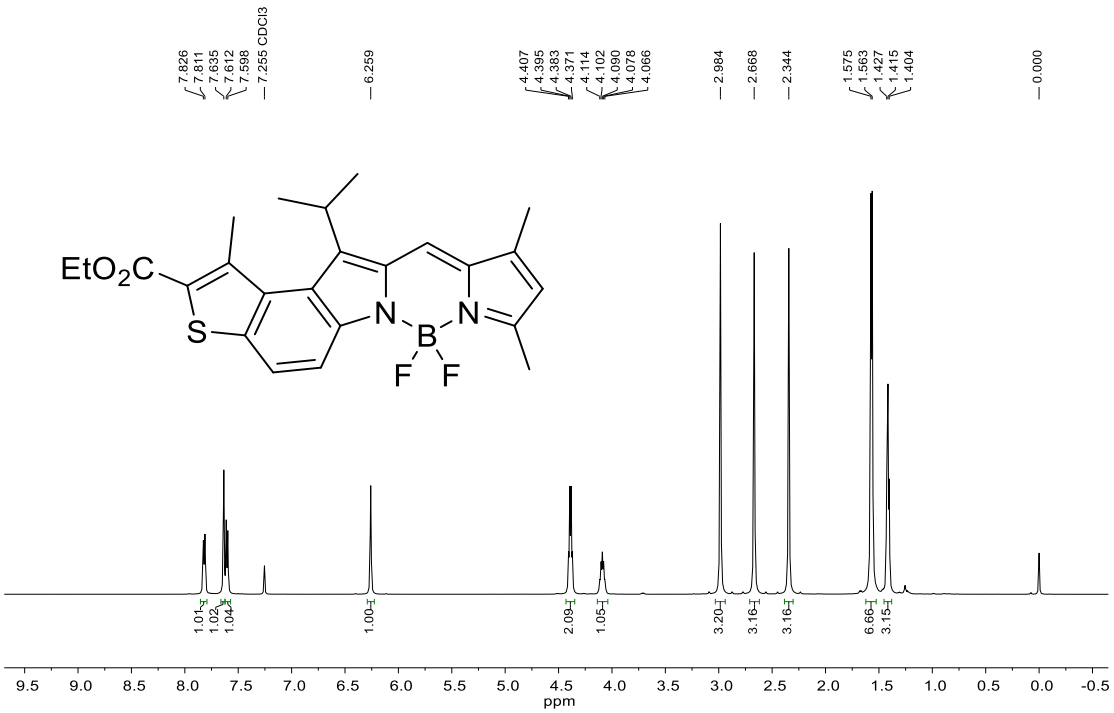


$^{1}$H NMR spectrum of **BBDP 1a** in $CDCl_3$

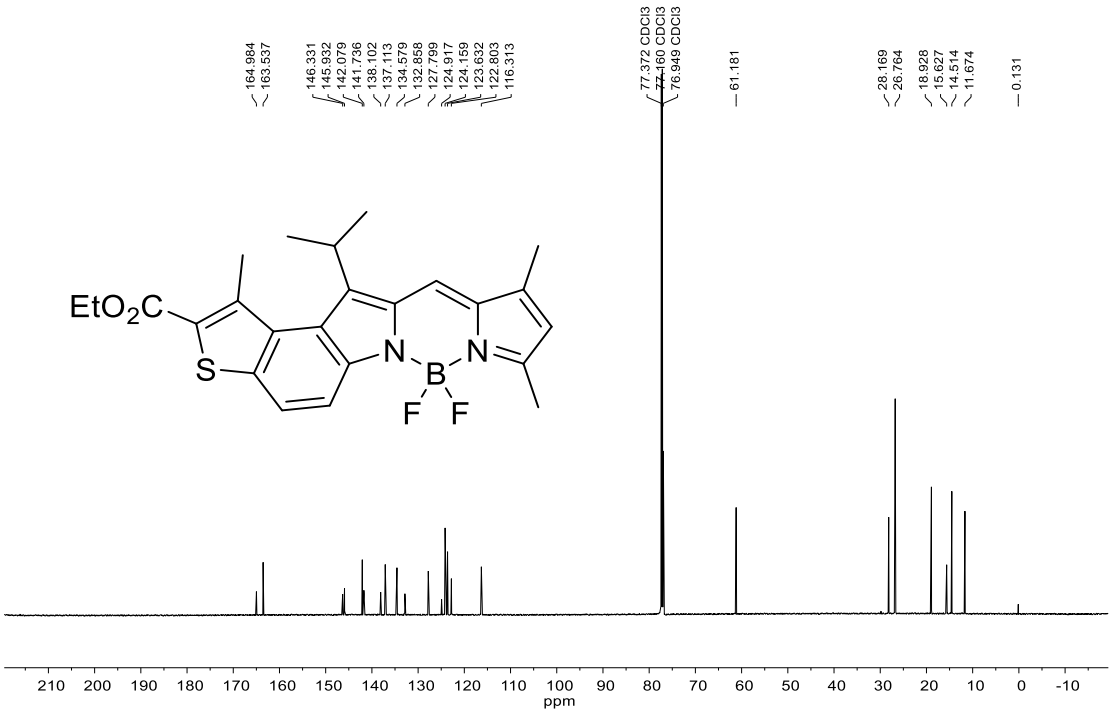


$^{13}$C NMR spectrum of **BBDP 1a** in $CDCl_3$

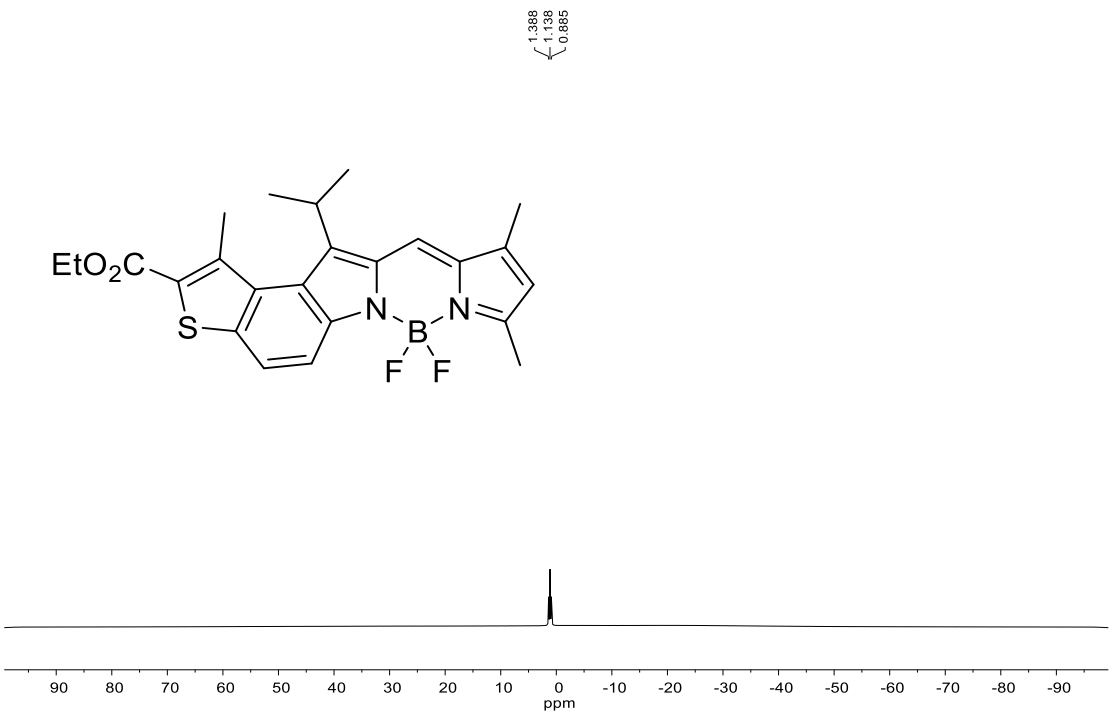


$^{11}$B NMR spectrum of **BBDP 1a** in $CDCl_3$

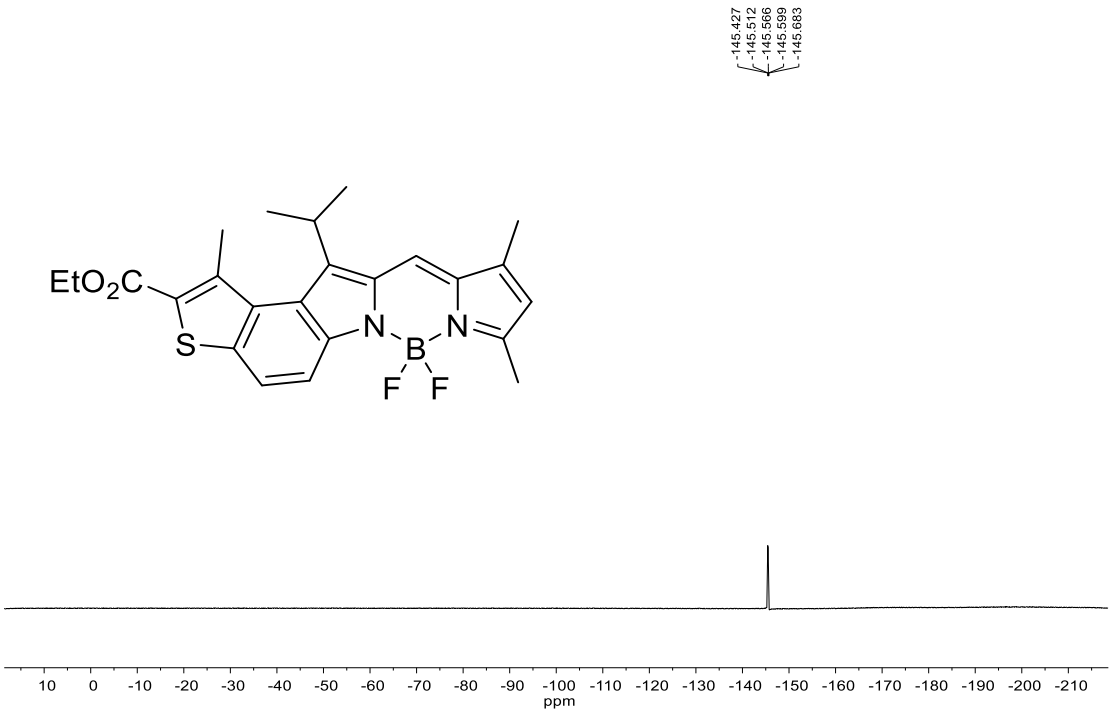


$^{19}$F NMR spectrum of **BBDP 1a** in $CDCl_3$

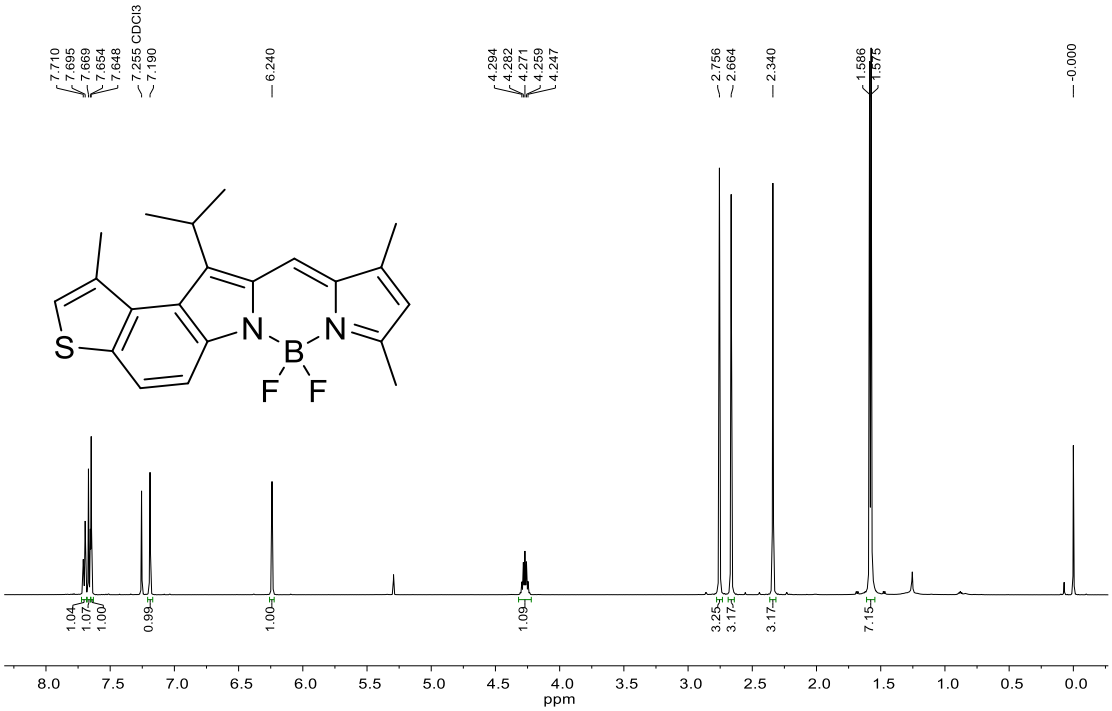


$^{1}$H NMR spectrum of **BBDP 1b** in $CDCl_3$

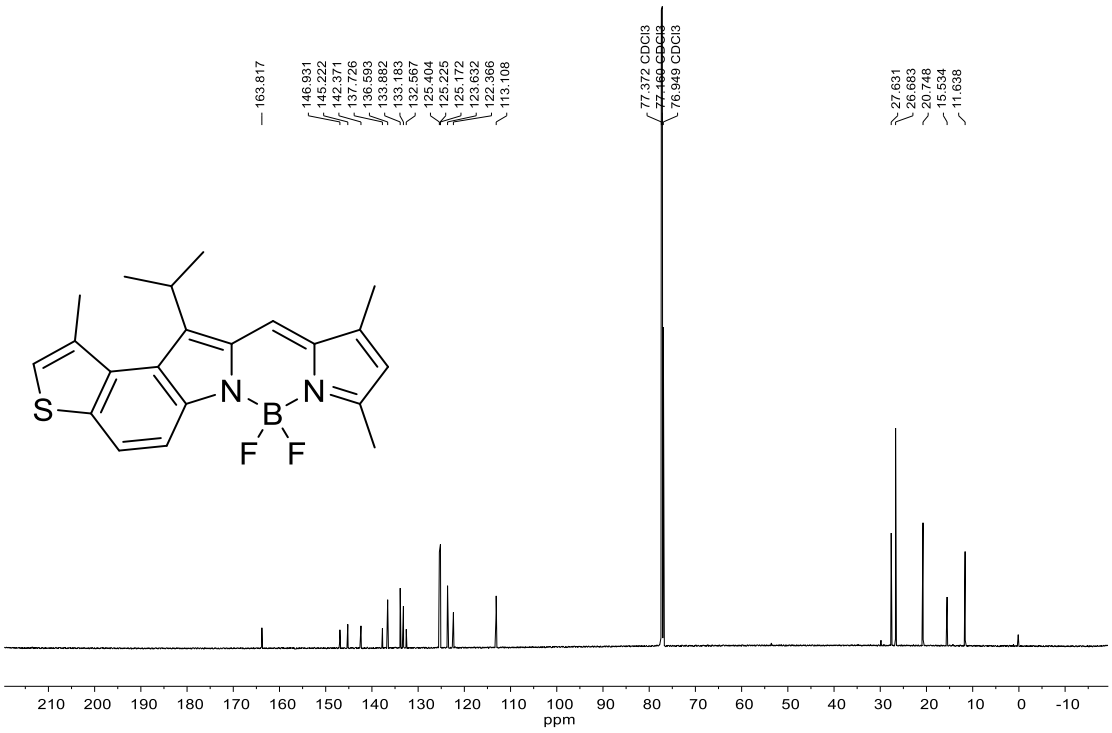


$^{13}$C NMR spectrum of **BBDP 1b** in $CDCl_3$

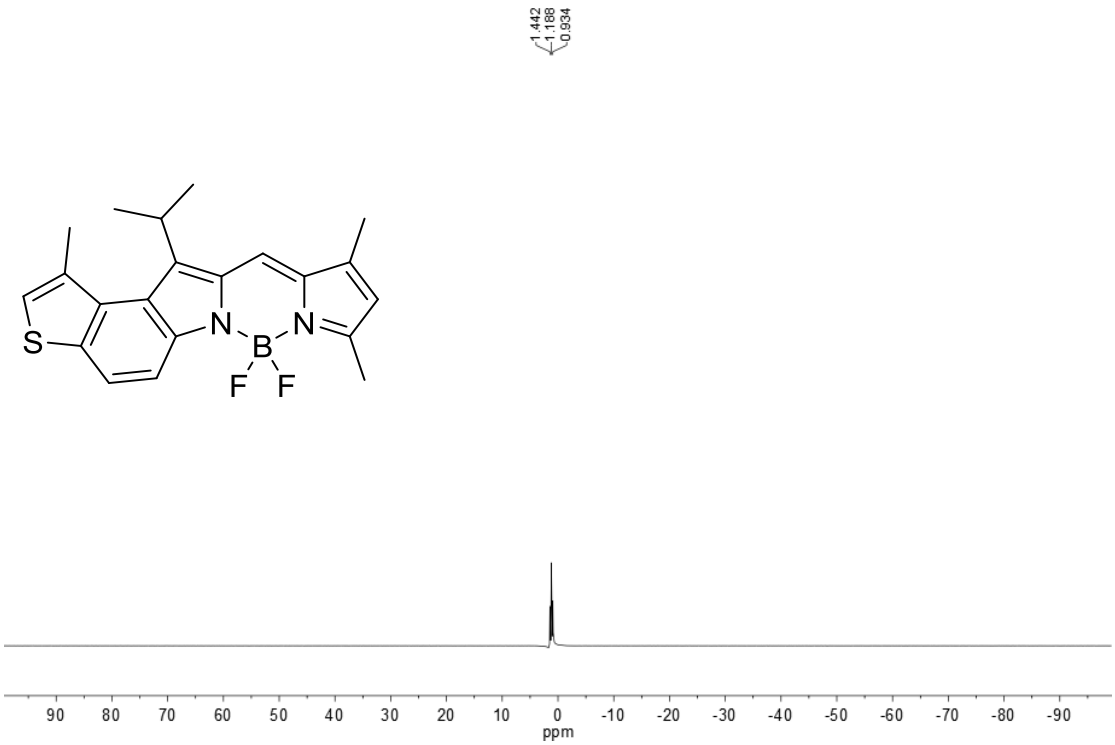


$^{11}$B NMR spectrum of **BBDP 1b** in $CDCl_3$

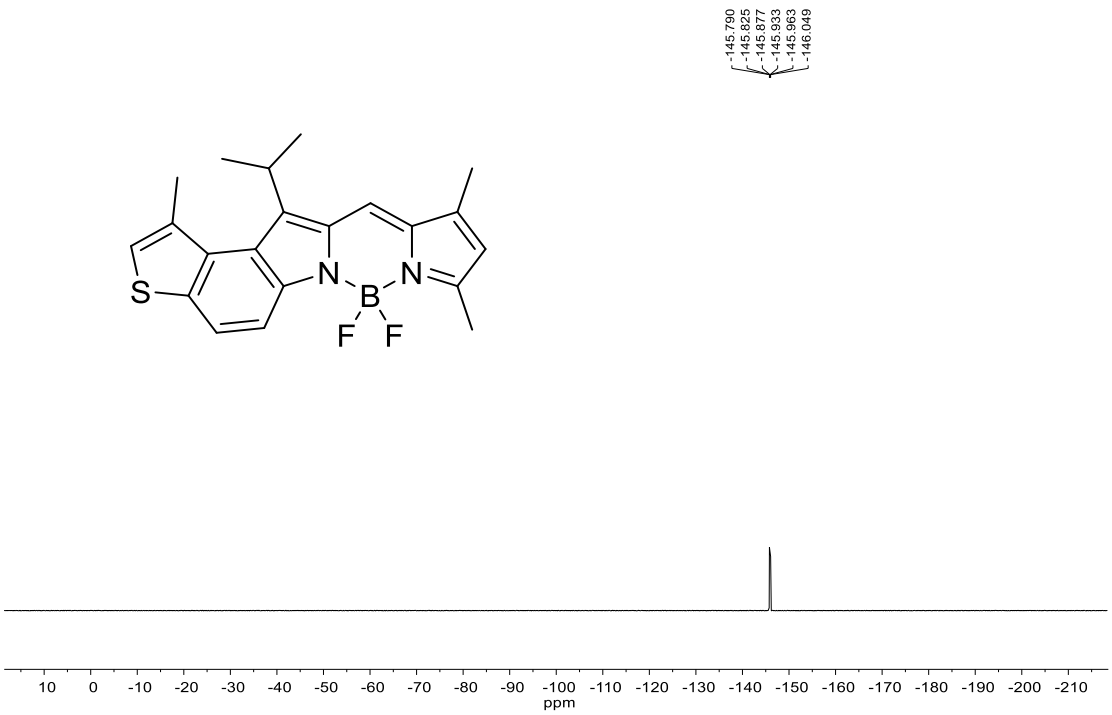


$^{19}$F NMR spectrum of **BBDP 1b** in $CDCl_3$

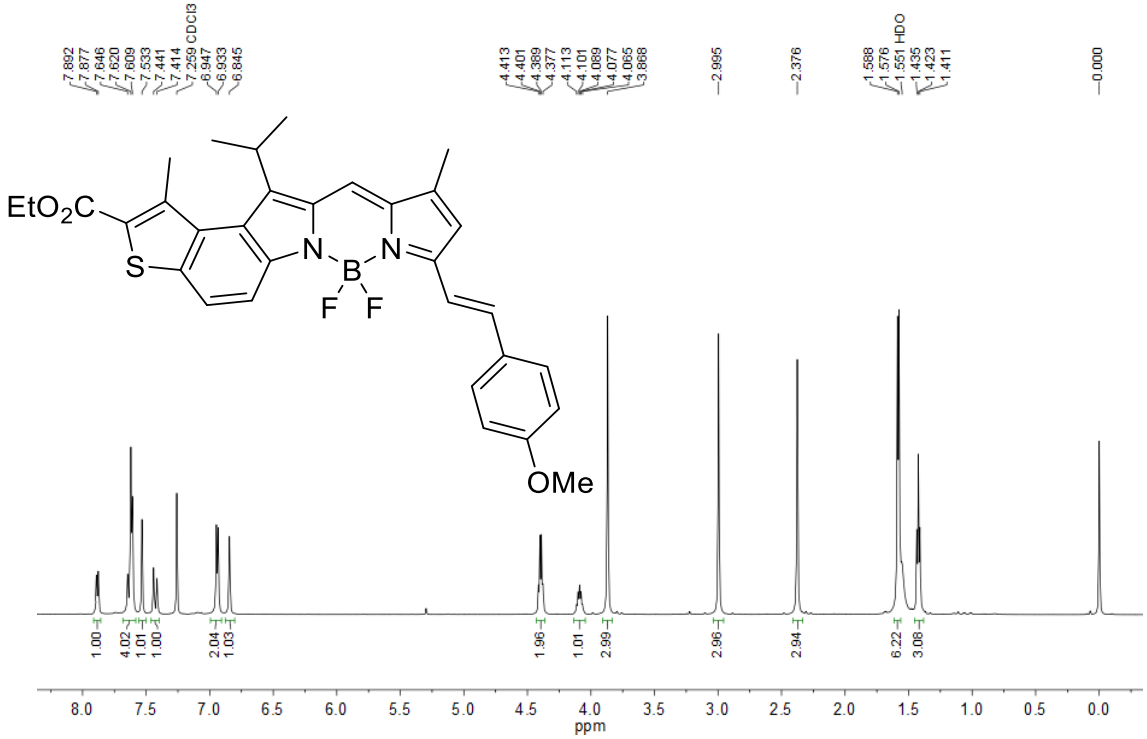


$^{1}$H NMR spectrum of **BSBDP 2a** in $CDCl_3$

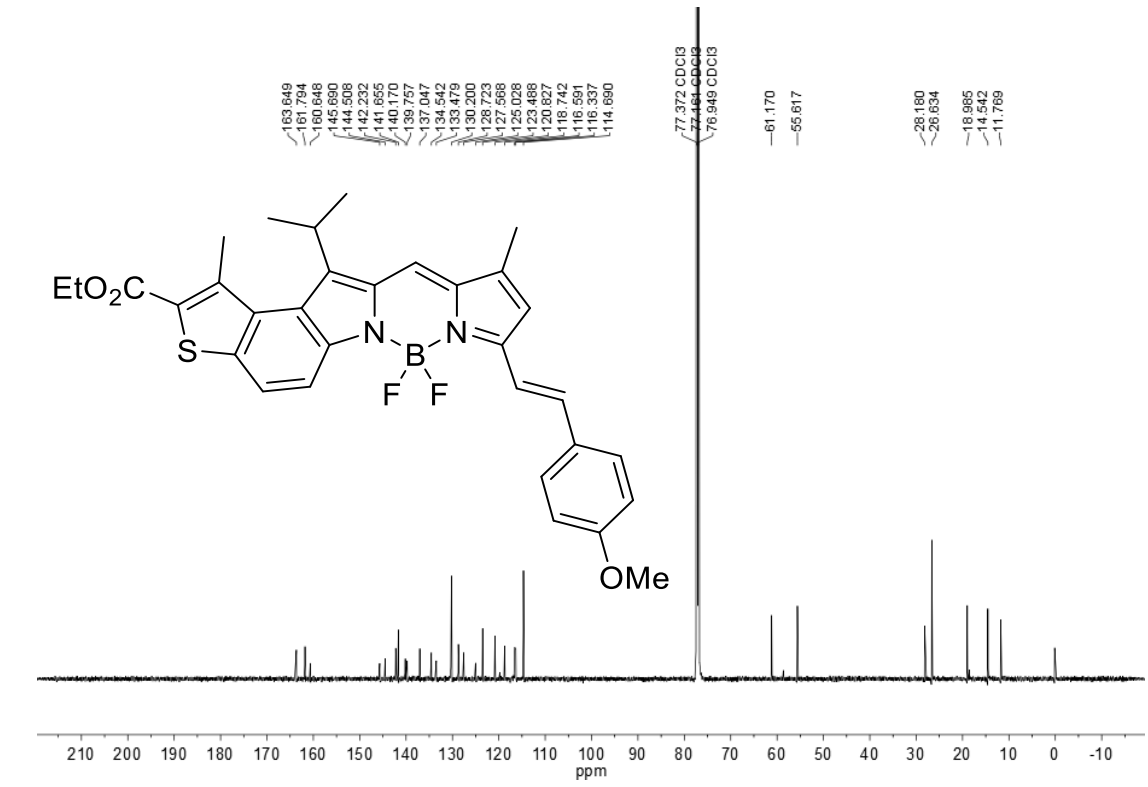


$^{13}$C NMR spectrum of **BSBDP 2a** in $CDCl_3$

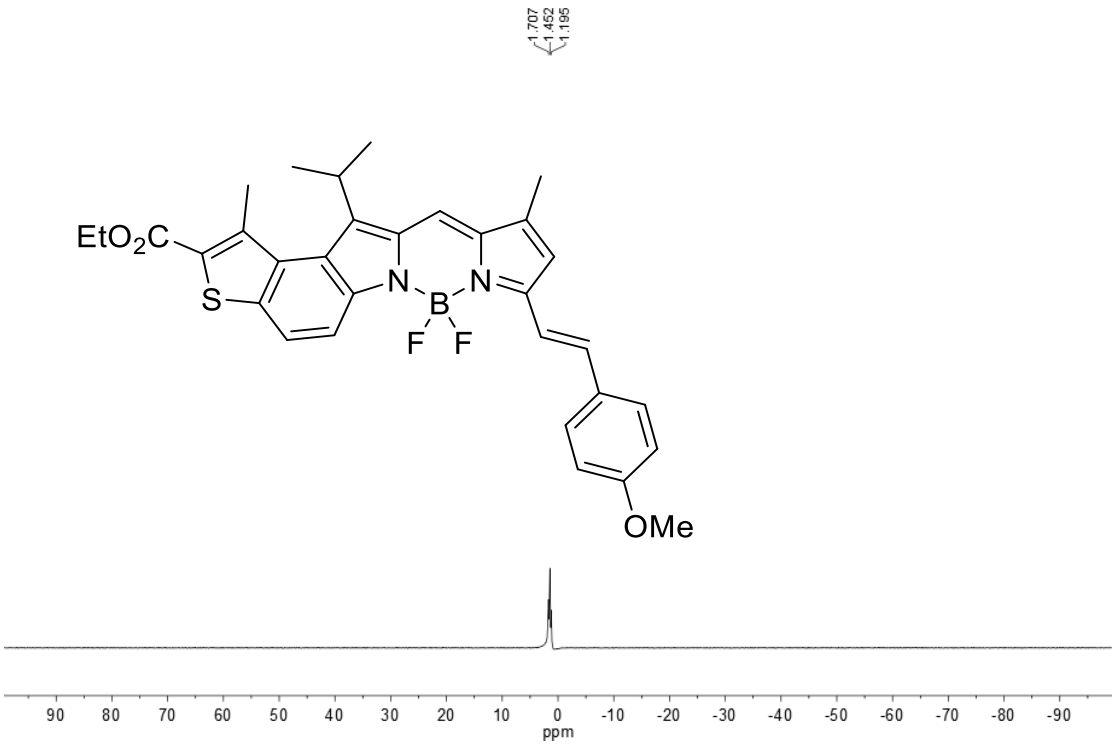


$^{11}$B NMR spectrum of **BSBDP 2a** in $CDCl_3$

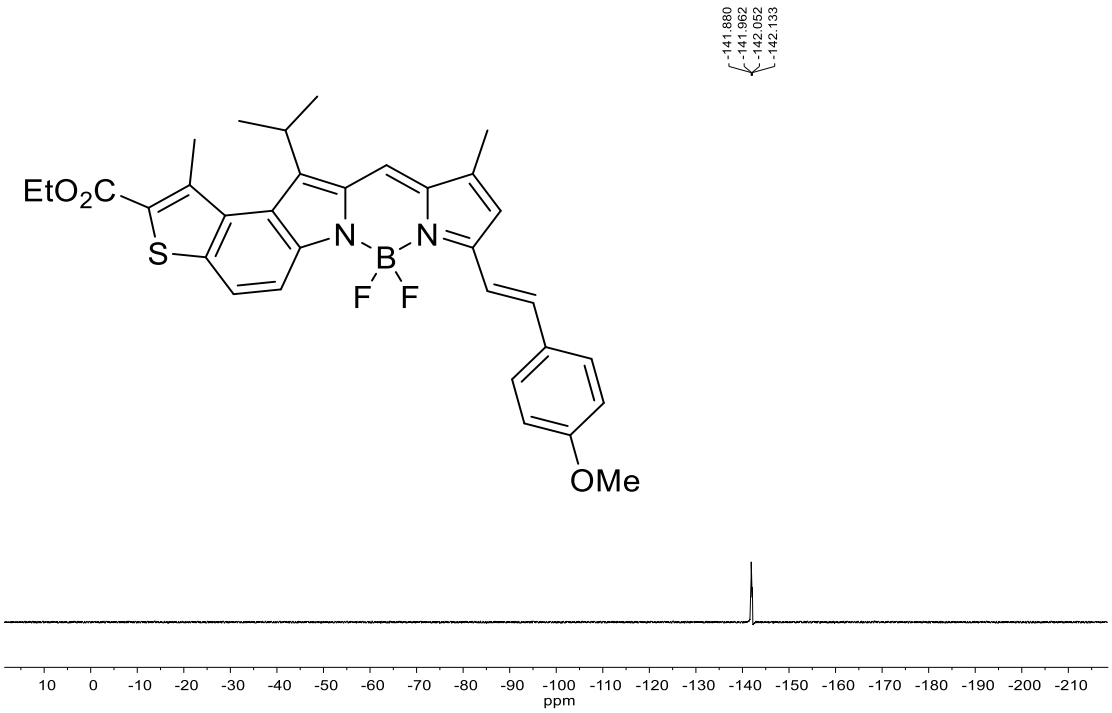


$^{19}$F NMR spectrum of **BSBDP 2a** in $CDCl_3$

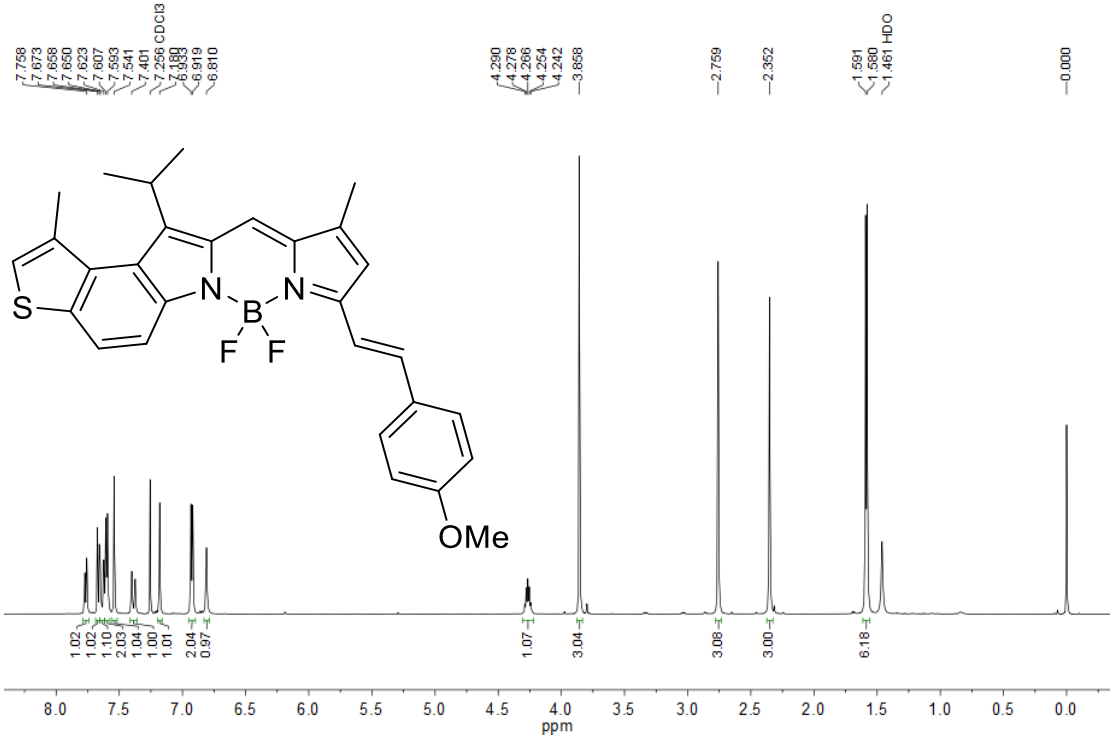


$^{1}$H NMR spectrum of **BSBDP 2b** in $CDCl_3$

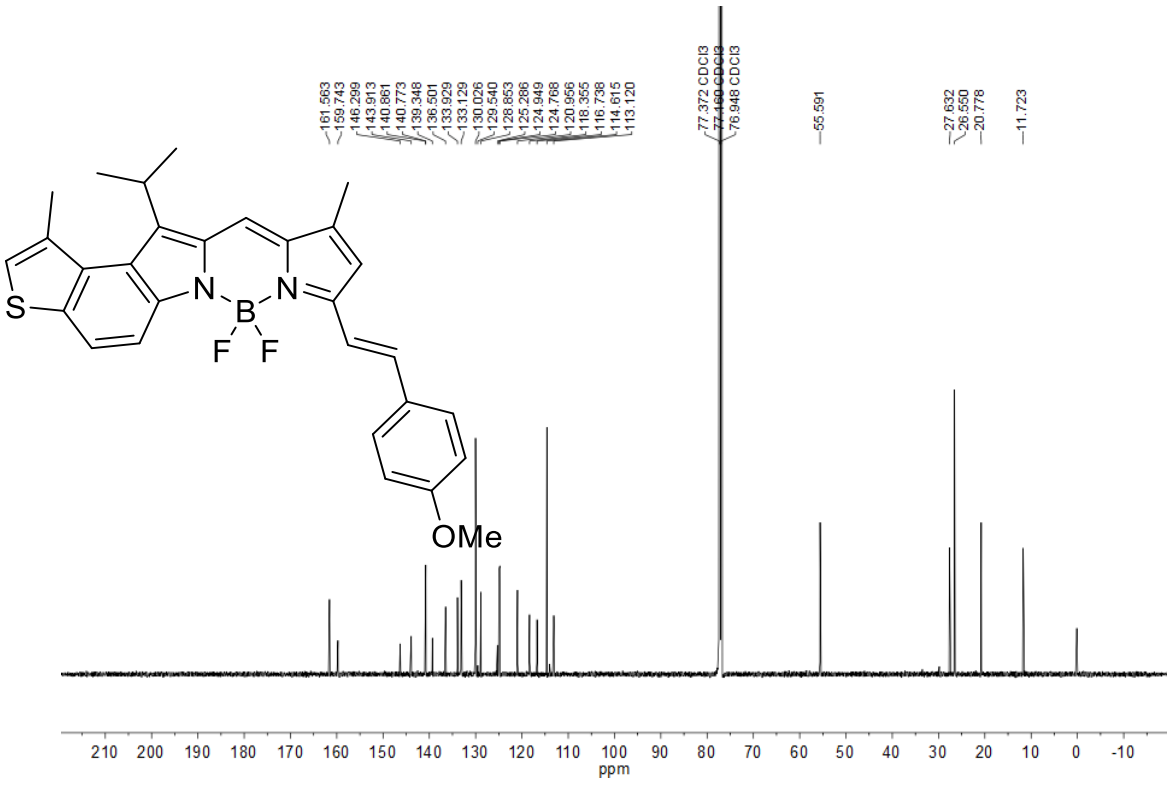


$^{13}$C NMR spectrum of **BSBDP 2b** in $CDCl_3$

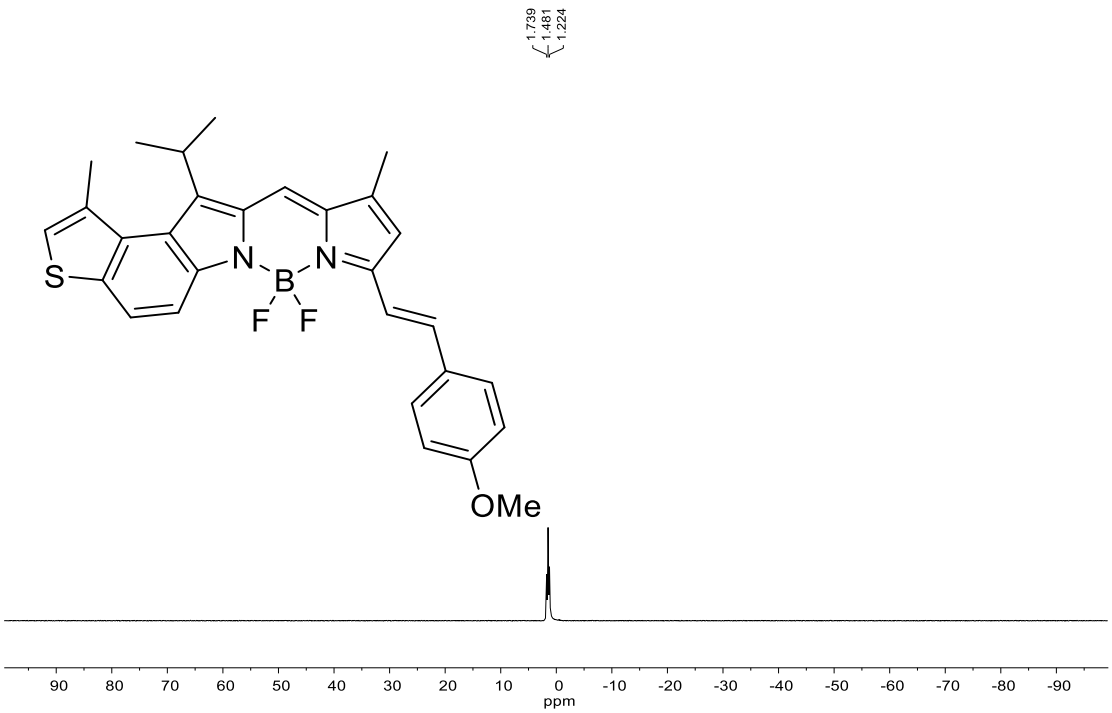


$^{11}$B NMR spectrum of **BSBDP 2b** in $CDCl_3$

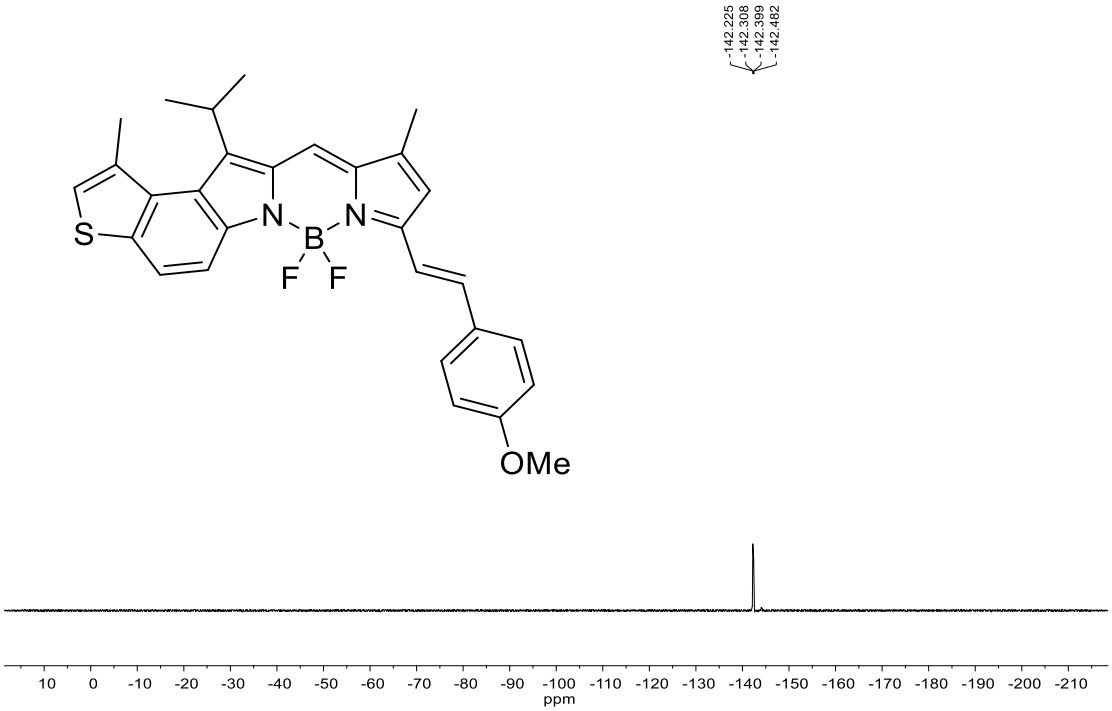


$^{19}$F NMR spectrum of **BSBDP 2b** in $CDCl_3$

# 10. HRMS spectra for all the new compounds

**HRMS for 3a**

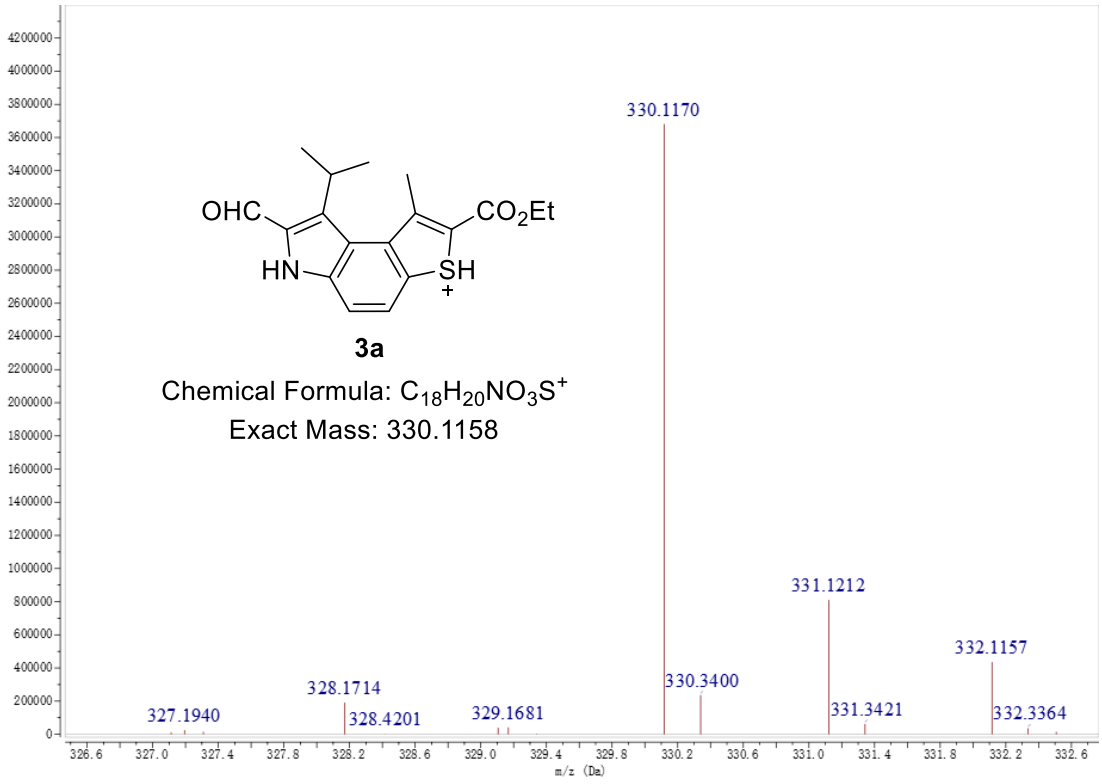


**HRMS for 3b**

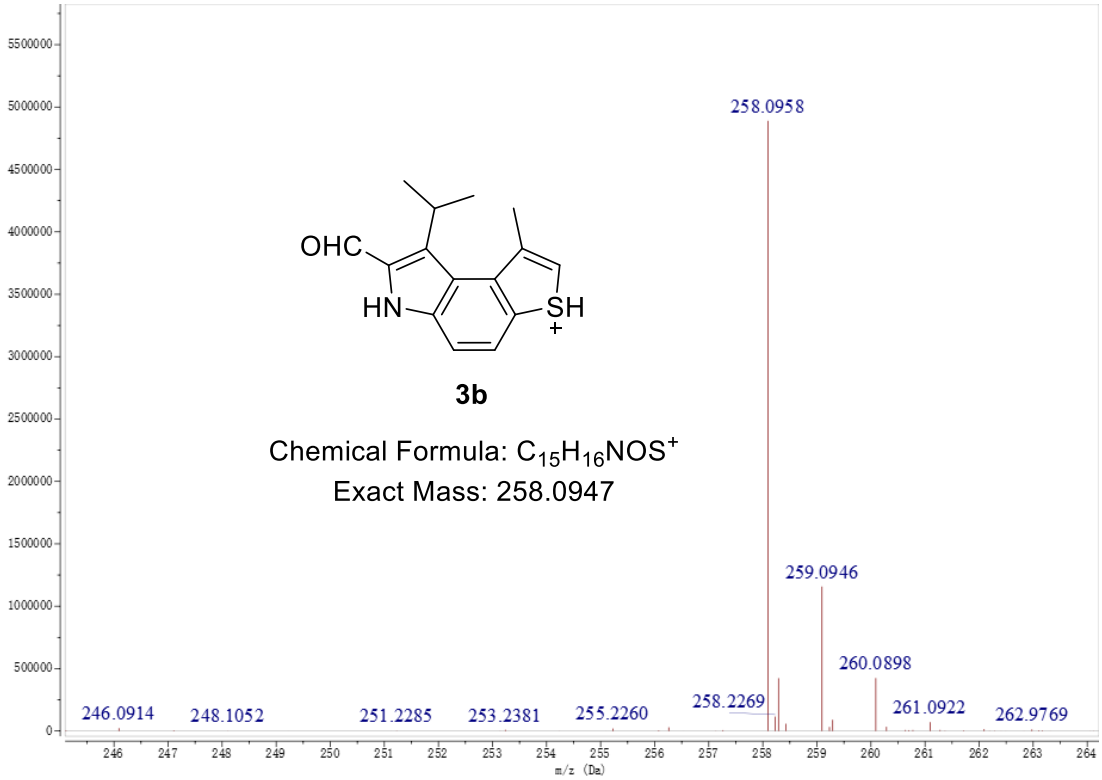

**HRMS for BBDP 1a**

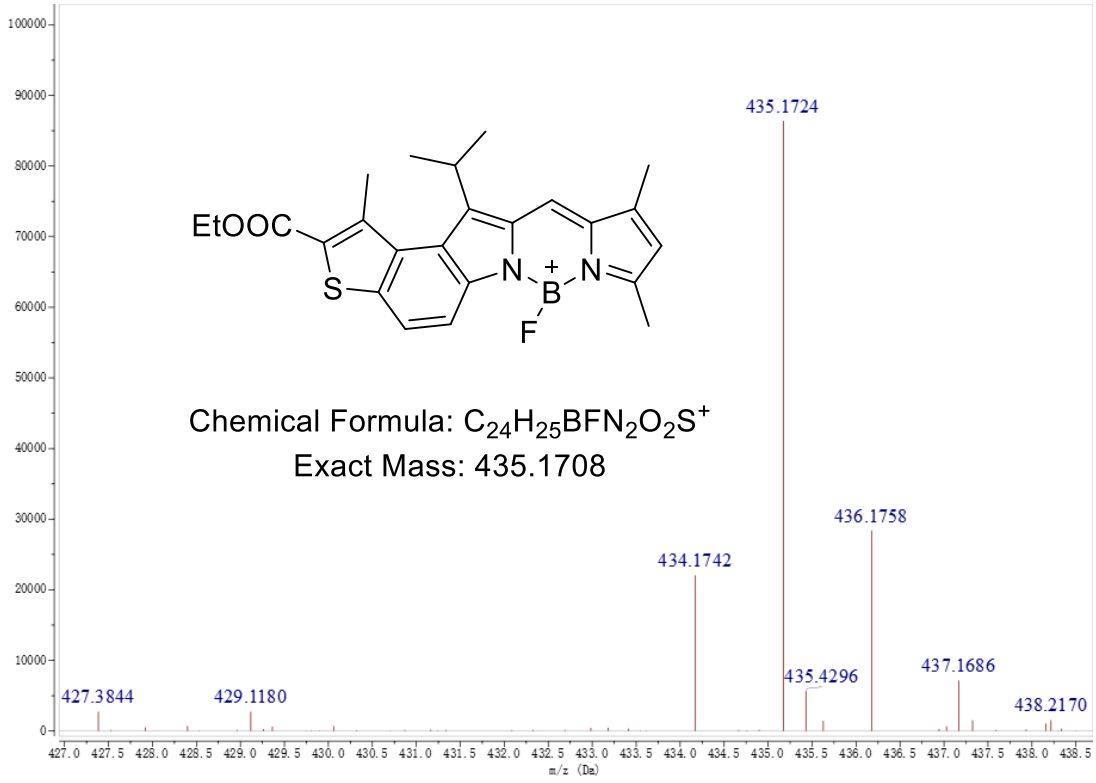


**HRMS for BBDP 1b**

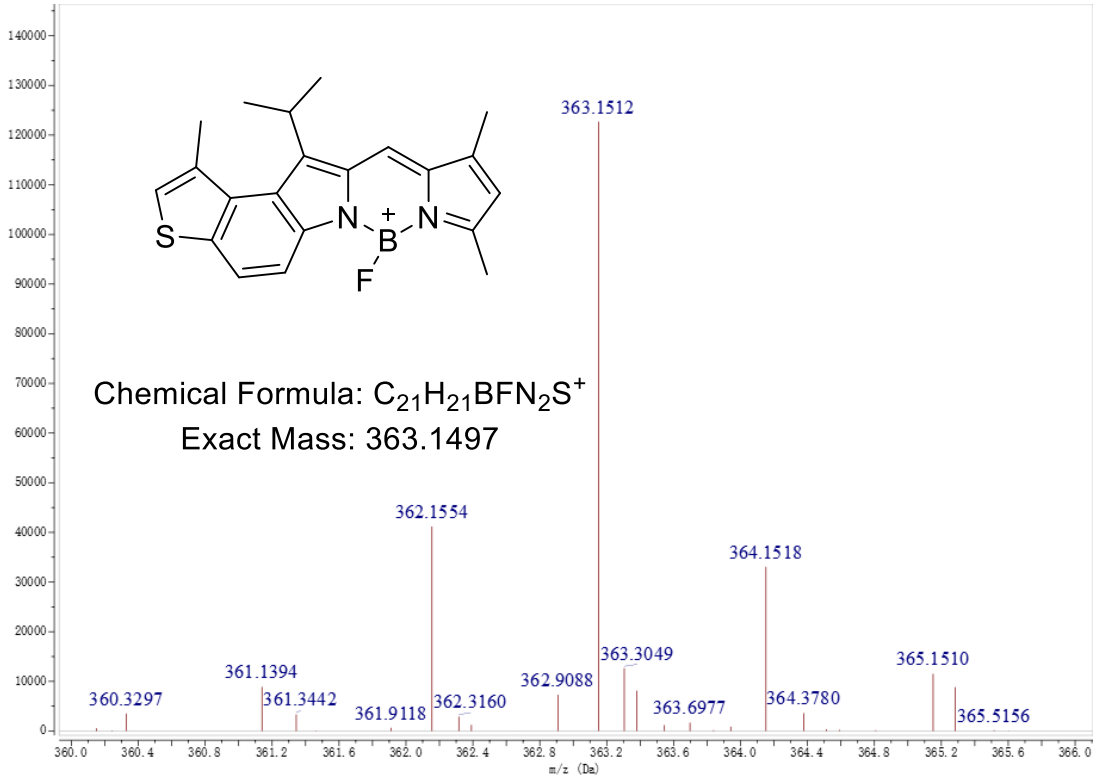

**HRMS for BSBDP 2a**

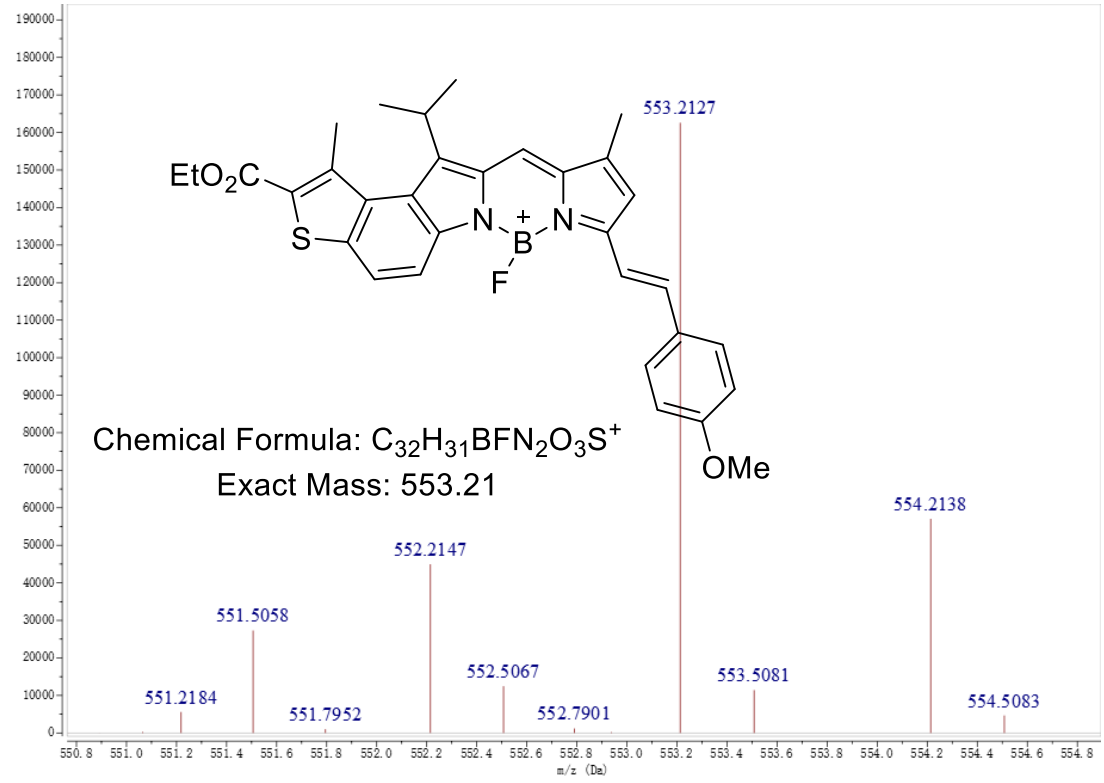


**HRMS for BSBDP 2b**

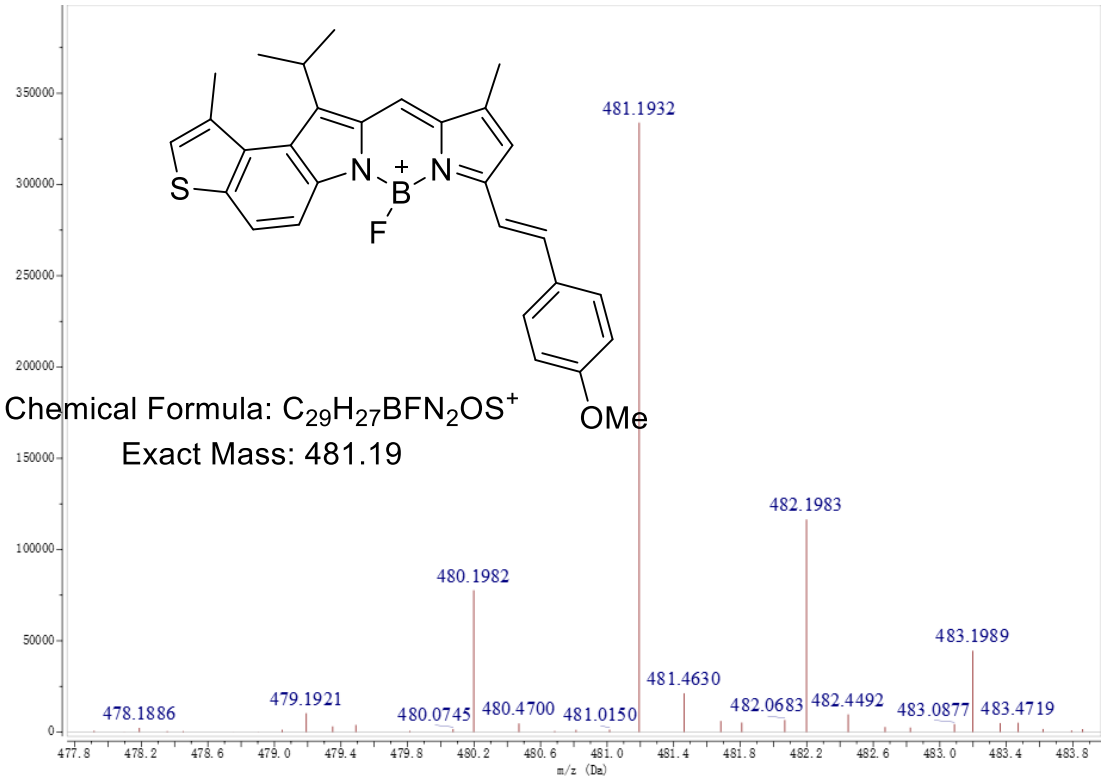

## 11. Author contribution statement

Weibin Bu: Investigation, data testing, validation, editing.

Changjiang Yu: supervision, writing, reviewing, funding acquisition.

Yingxiu Man: Data testing.

Jiazhu Li: Reviewing, supervision.

Qinghua Wu: Carried out theoretical calculations, Writing about theoretical calculations.

Shuangying Gui: Investigation about in vivo bioimaging, data testing, Reviewing

Yaxiong Wei: Reviewing, supervision.

Lijuan Jiao: Reviewing.

Erhong Hao: Funding acquisition, validation, reviewing, supervision.

## 12. References

[1]. Y. Kawamura, H. Sasabe and C. Adachi, Jpn. *J. Appl. Phys*., 2004, **43**, 7729.

[2] Z. Feng, Y. Feng, C. Yu, N. Chen, Y. Wei, X. Mu, L. Jiao and E. Hao, *J. Org. Chem*., 2016, **81**, 6281.

[3] a) Z. Lou, Y. Hou, K. Chen, J. Zhao, S. Ji, F. Zhong, Y. Dede and B. Dick, *J. Phys. Chem. C.*, 2018, **122**, 185; b) Z. Wang, J. Zhao, A. Barbon, A. Toffoletti, Y. Liu, Y. An, L. Xu, A. Karatay, H. G. Yaglioglu, E. A. Yildiz, M. Hayvali, *J. Am. Chem. Soc.*, 2017, **139**, 783; c) Y. Hou, J. Liu, N. Zhang and J. Zhao, *J. Phys. Chem. A* 2020, **124**, 9360.

[4] Y.-C. Lai, S.-Y. Su and C.-C. Chang, *ACS Appl. Mater. Interfaces*, 2013, **5**, 12935.

[5] Y. Zhu, C. Chen, G. Yang, Q. Wu, J. Tian, E. Hao, H. Cao, Y. Gao, W. Zhang, *ACS Appl. Mater. Interfaces* 2020, **12**, 44523.

[6] X. Guo, J. Yang, M. Li, F. Zhang, W. Bu, H. Li, Q. Wu, D. Yin and E. Hao, *Angew. Chem. Int. Ed.*, 2022, **61**, e202211081.

[7] U. Mayerhöffer, F. Würthner, *Chem. Sci.*, 2012, **3**, 1215.

[8] Gaussian 09, Revision D.01, M. J. Frisch, G. W. Trucks, H. B. Schlegel, G. E. Scuseria, M. A. Robb, J. R. Cheeseman, G. Scalmani, V. Barone, B. Mennucci, G. A. Petersson, H. Nakatsuji, M. Caricato, X. Li, H. P. Hratchian, A. F. Izmaylov, J. Bloino, G. Zheng, J. L. Sonnenberg, M. Hada, M. Ehara, K. Toyota, R. Fukuda, J. Hasegawa,

M. Ishida, T. Nakajima, Y. Honda, O. Kitao, H. Nakai, T. Vreven, J. A. Montgomery, Jr., J. E. Peralta, F. Ogliaro, M. Bearpark, J. J. Heyd, E. Brothers, K. N. Kudin, V. N. Staroverov, T. Keith, R. Kobayashi, J. Normand, K. Raghavachari, A. Rendell, J. C. Burant, S. S. Iyengar, J. Tomasi, M. Cossi, N. Rega, J. M. Millam, M. Klene, J. E. Knox, J. B. Cross, V. Bakken, C. Adamo, J. Jaramillo, R. Gomperts, R. E. Stratmann, O. Yazyev, A. J. Austin, R. Cammi, C. Pomelli, J. W. Ochterski, R. L. Martin, K. Morokuma, V. G. Zakrzewski, G. A. Voth, P. Salvador, J. J. Dannenberg, S. Dapprich, A. D. Daniels, O. Farkas, J. B. Foresman, J. V. Ortiz, J. Cioslowski, and D. J. Fox, Gaussian, Inc., Wallingford CT, 2013.